BAS

Sensor Notes

Note 4

August 1982

THE FREQUENCY DOMAIN REFLECTOMETER (FDR) -- PHASE I: CONCEPT VERIFICATION

Neal P. Baum
NMERI
University of New Mexico
Box 25, University Station
Albuquerque, New Mexico 87131

Carl E. Baum
Air Force Weapons Laboratory (NTYE)
Kirtland Air Force Base, New Mexico 87117

Thomas O Summers and Garland W. Fulton
Summers Engineering, Incorporated
215 Sierra Drive SE
Albuquerque, New Mexico

ABSTRACT

The initial development of a new high stress particle motion gage is described. The gage uses a low frequency (500 kHz) a.c. technique to measure the self-inductance of a coaxial cable segment. The self-inductance is proportional to the cable's length. It thus measures particle displacement. A quadrature technique is used to measure both the inductance and resistance of the coax. The resistance can be used to correct the inductance measurement. However, in the high explosive (HE) testing that was done, the conductivity did not perturb the inductance measurement. This was true for both grout and epoxy dielectrics. The peak pressures achieved in the grout were of the order of 10 GPa.

CONTENTS

I. INTRODUCTION

BACKGROUND

World War II and the Manhattan Project gave birth to the nuclear bomb. Since that time we in the instrumentation community have been trying to parameterize the bomb's effects to a greater degree of accuracy than that provided by Fermi's scraps of paper.* In the blast and shock case the result has been to bring the instrumentation closer and closer to the bomb itself. In the ground shock case the effect has been to develop gages that can survive for limited times at higher and higher stresses. The present capability is in the low gigapascal range. The desire is to attain limited survival at the moderate gigapascal range (30 GPa) in the associated radiation and Electromagnetic Pulse (EMP) environments.

One may logically ask that if no rational defense structure can survive the inputs, then why bother to develop such gages. Well, when a nuclear device is detonated it releases a great deal of energy in forms of radiation and kinetic energy associated with vaporized bomb debris and other local substances. If the burst is at or near the ground surface, a significant portion of the energy couples into the ground. At present the mechanisms of and the amount of energy coupling are not known. The calculators hypothesize but the empiricists require verification, for this knowledge is critical in determining the cratering effectiveness of the device, which is in turn a necessary input to those designing hardened strategic systems or devices used to attack these types of systems.

Recognizing this problem the Air Force Weapons Laboratory (AFWL) proposed a series of underground tests in the early seventies. These were called CAvity Nuclear Tests (CANT). These tests consisted of shots using small devices in relatively large underground hemispherical cavities. The purpose was to simulate the early time environment of a surface nuclear burst. The basic requirement for the instrumentation was to be able to measure stress and particle velocity close in to the device. In spite of an ongoing instrumentation program sponsored by the Defense Nuclear Agency (DNA), the instrumentation

---

*Enrico Fermi (1901-1954), Italian-born American physicist. Research on producing radioactive isotopes by neutron bombardment; directed construction of the first atomic pile; Nobel Prize, 1938.

community was not ready for CANT. As Reference 1 explains, the instrumentation did not exist at the time in a stage of development suitable to meet the objectives of CANT. After CANT went by the wayside, other possible large cavity shots were considered to determine if this need could be fulfilled. While each of these shots has a different systems-related justification, each one is basically a small device in a relatively large underground hemispherical cavity, and once again the opportunity was presented for close-in motion and stress measurements.

The basic requirement is that the stress and particle velocity be measured for given periods of time at locations where different peak stresses are expected. The gages should survive for 200 μs at 30 GPa and 300 μs at 3 GPa. This has required a continuation of the high stress instrumentation development program sponsored by DNA. The gage described here is part of that program.

The Frequency Domain Reflectometer (FDR) came about as one of the recommendations of a joint AFWL/Research and Development Associates (RDA) committee tasked with reviewing the current state of the art in high stress measurements and making recommendations for future development. Since one of the concerns was electrical noise on the measurements, the committee was made up of one member of the EMP community from each organization and one member of the blast and shock instrumentation community from or representing each organization. One of the recommendations is contained in Reference 2 which describes the parameters relevant to using the inductance of transmission lines to determine the position of the lines' end points. The subsequent section is, for the most part, a summary of the relevant points contained in that document.

GAGE THEORY

Before proceeding with a discussion of transmission line characteristics, it is instructive to discuss the philosophy associated with gage design. It

---

1. Baum, N. P., *Instrumentation Evaluation for Surface Bursts in Underground Cavities*, BAS Sensor Notes, Note 1, June 1973.
2. Baum, C. E., *Inductive Techniques Using Uniform Transmission-Line Structures for Measuring Eulerian Position in Langragian-Flow Shock Waves in High-Density Media*, BAS Sensor Notes, Note 2, September 1978.

is important that the measurand of interest not be significantly perturbed by other medium parameters, particularly by those parameters which may also be changing in the shock environment. To the extent that these other parameters are uncertain, the results of the measurement will be uncertain.

All the techniques under consideration locate the position or velocity of some conducting plate by either scattering electromagnetic fields off the plate or measuring those emanating from the plate. All the sensors are embedded in some medium, be it a separate internal dielectric or the surrounding medium itself. This medium transmits the electromagnetic fields (incident plus scattered). It is important that the electrical properties of the medium (including changes under high-pressure conditions) do not significantly affect the sensor's performance. Therefore the sensor must be insensitive to the changing electrical parameters of the medium (permittivity ε and conductivity σ), but the sensor can use the magnetic properties of the medium (permeability μ) since we assume that

$$\mu \simeq \mu_0 \text{ (permeability of free space)} \tag{1}$$

even under high-pressure conditions. Thus, given the choice, the experimenter should opt for magnetic coupling as opposed to electrical coupling. In general, we allow

$$\overleftrightarrow{\varepsilon} = \overleftrightarrow{\varepsilon}(\vec{r},t) \quad \text{(dyadic permittivity)}$$
$$\overleftrightarrow{\sigma} = \overleftrightarrow{\sigma}(\vec{r},t) \quad \text{(dyadic conductivity)} \tag{2}$$

i.e., dyadic functions of space $\vec{r} = (x,y,z)$ and time t for the electrical conditions.

Another requirement is that the conductors used should be mechanically as close in impedance to the media as practical. Beryllium, magnesium, and aluminum are three possible candidates that are listed in order of increasing practicality. However, since there will always be some mechanical mismatch the mass and volume of conductors should be kept to a minimum, consistent with rational survival under shock conditions.

Following Reference 2, consider schematically a transmission line of length $\ell(t)$ which varies slowly as a function of t (Fig. 1). Changes are associated with the deformation of the medium for which the associated shock velocity (velocities), v_s, is small compared to the speed of light in a vacuum, c, or in the medium, v. The transmission line has a characteristic impedance, $\tilde{Z}$, where

$$\tilde{Z}_c = \tilde{Z}_c(z,s) = f_g(z)\,\tilde{Z}(z,s)$$

$f_g(z) \equiv$ dimensionless geometrical factor

$z \equiv$ coordinate along transmission line

$$\tilde{Z}(z,s) = \left[\frac{\tilde{\sigma}(z,s) + s\tilde{\varepsilon}(z,s)}{s\mu_0}\right]^{\frac{1}{2}}$$

$\equiv$ wave impedance of ambient medium

$\tilde{\sigma}(z,s) \equiv$ conductivity of ambient medium (assumed a scalar)

$\tilde{\varepsilon}(z,s) \equiv$ permittivity of ambient medium (assumed a scalar)

$\mu_0 \equiv 4\pi \times 10^{-7}\ \frac{H}{m}$

$\equiv$ permeability of free space

$=$ permeability of ambient medium (3)

In another form, this is

$$\tilde{Z}_c(z,s) = \left[\frac{sL'(z)}{\tilde{G}'(z,s) + s\tilde{C}'(z,s)}\right]^{\frac{1}{2}}$$

$L'(z) = \mu_0 f_g(z) \equiv$ inductance per unit length

$\tilde{C}'(z,s) = \frac{\tilde{\varepsilon}(z,s)}{f_g(z)} \equiv$ capacitance per unit length

$\tilde{G}'(z,s) = \frac{\tilde{\alpha}(z,s)}{f_g(z)} \equiv$ conductance per unit length (4)

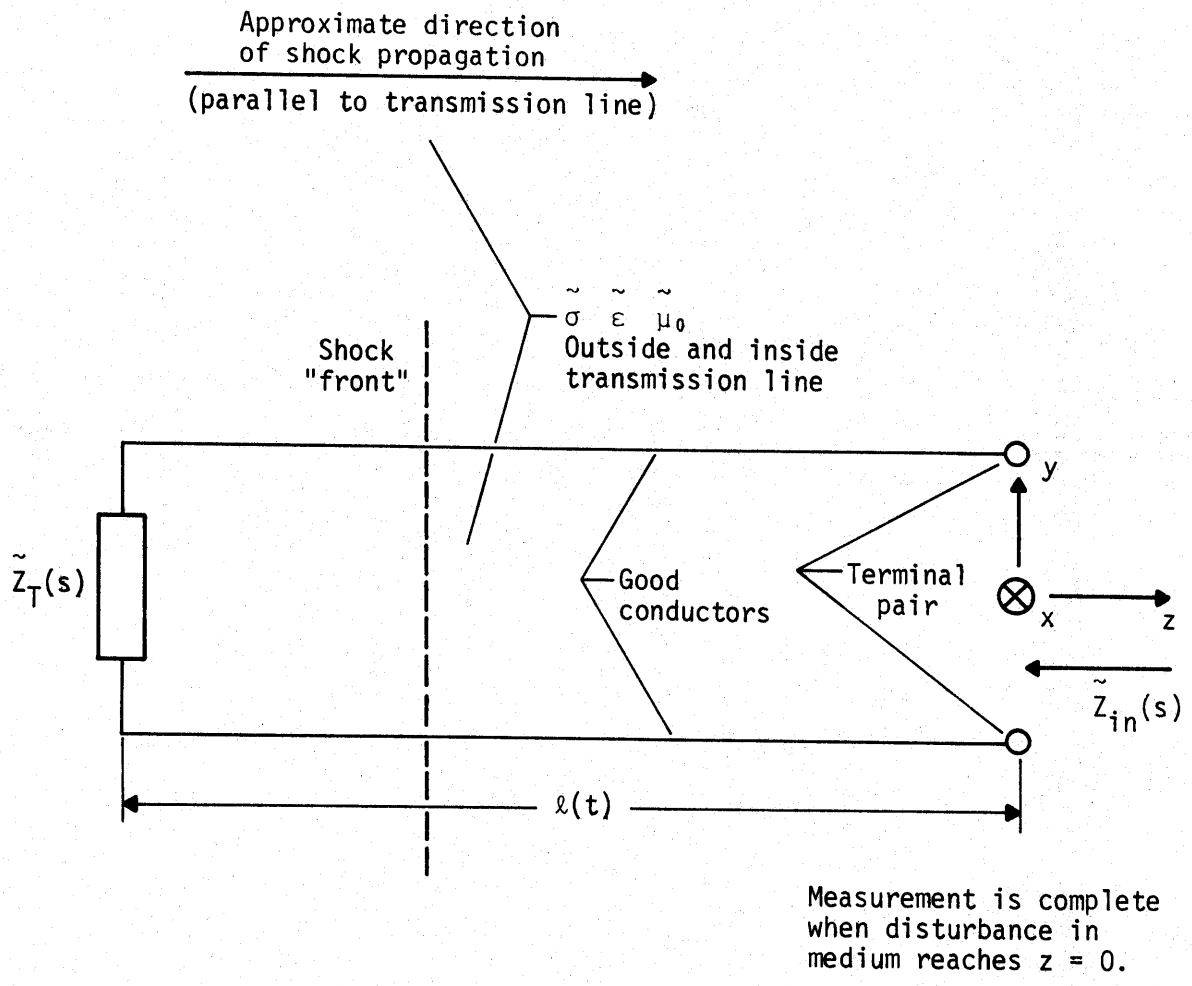

Figure 1. Transmission line with axis parallel to shock propagation in ambient medium.

In terms of these same parameters, the propagation constant is

$$\tilde{\gamma}(z,s) = \left\{ s\mu_0 [\tilde{\sigma}(z,s) + s\tilde{\varepsilon}(z,s)] \right\}^{\frac{1}{2}}$$

$$= \left\{ sL'(z)[\tilde{G}'(z,s) + s\tilde{C}'(z,s)] \right\}^{\frac{1}{2}} \qquad (5)$$

Note that the electromagnetic properties of the medium that are changed under the shock conditions can in general be a function of both position, z, and complex frequency, s. They may also be functions of time, t, because of the changes induced in the medium, but these changes are assumed low compared to times required for the electromagnetic processes to achieve a steady state. Where required, the electromagnetic influence of these changes in the ambient medium can be introduced as perturbations.

In the case where the length, ℓ, of the transmission lines is small compared to the wavelength of the excitation signal, the expression for the input impedence ($Z_{in}(s)$) reduces to

$$Z_{in}(s) = sL \frac{1 + \frac{1}{6}[\tilde{\gamma}(s)\ell]^2 + 0\left\{[\tilde{\gamma}(s)\ell]^4\right\}}{1 + \frac{1}{2}[\tilde{\gamma}(s)\ell]^2 + 0\left\{[\tilde{\gamma}(s)\ell]^4\right\}} \qquad (6)$$

$L \equiv L'\ell \equiv$ transmission-line inductance

This says that a shorted transmission line (with lossless conductors) placed in the ambient medium and electrically exposed to the medium has an inductive impedance at low frequencies, this low frequency impedance being independent of both the conductivity and the permittivity of the medium.

To explore the implications of Equation 6 further, the numerator and denominator series expansions are combined as

$$\tilde{Z}_{in}(s) = sL\left[1 + \frac{1}{3}\tilde{\Gamma}^2 + 0(\tilde{\Gamma}^4)\right]$$

$$= sL\left(1 - \frac{1}{3} s\mu_0 \ell[\tilde{\sigma}(s) + s\tilde{\varepsilon}(s)]\ell + 0\,[\tilde{\Gamma}^4]\right)$$

$$= sL\left(1 - \frac{1}{3} sL[\tilde{G}'(s)\ell + s\tilde{C}'(s)]\ell + 0\,[\tilde{\Gamma}^4]\right. \qquad (7)$$

where

$$\tilde{\Gamma} = \tilde{\gamma}(s)\ell$$

This gives a correction term indicating how much the conductivity and permittivity can change the input impedance. Rewriting Equation 7 as

$$\tilde{Z}_{in}(s) = sL\left\{1 + \tilde{\Delta}(s) + 0\left([\tilde{\gamma}(s)\ell]^4\right)\right\}$$

$$= s\mu_0 \ell f_g\left\{1 + \tilde{\Delta}(s) + 0\left([\tilde{\gamma}(s)\ell]^4\right)\right\} \tag{8}$$

the first-order $\tilde{\Delta}$ is

$$\tilde{\Delta}(s) = -\frac{1}{3} s\mu_0 \ell[\tilde{\sigma}(s) + s\tilde{\varepsilon}(s)]\ell$$

$$= -\frac{1}{3} sL[\tilde{G}'(s)\ell + s\tilde{C}'(s)\ell] \tag{9}$$

One criterion for an accurate measurement is that $|\tilde{\Delta}| << 1$. Since at low frequencies $\tilde{\Delta}(s) \to 0$ as $s \to 0$, this criterion is consistent with the prior considerations which argued toward a low-frequency measurement. Now one has some estimate of "how low is low." As an example, let

$$\sigma \equiv 10^{-2} \frac{S}{m}$$

$$\varepsilon = 10\varepsilon_0 \simeq 0.885 \times 10^{-10} \frac{F}{m} \tag{10}$$

This corresponds to a not atypical soil or concrete (neglecting frequency dependence). Then, choosing a frequency of 500 kHz and a length of 1 m, the error is of the order of 1 percent.

It is also noted that at high pressures the medium may have a higher conductivity, thus limiting the gage length or lowering the excitation frequency.

There is also a restraint on the conductance of the metal path used to form the shorted transmission line. Basically this reduces to the fact that the resistance (R) must meet the following condition:

$$R << [|\tilde{G}'(s) + s\tilde{C}'(s)|\ell]^{-1} \tag{11}$$

This constraint says that ℓ should not be too large, and that the cross-section dimensions of the conductors (and their conductivities) should not be too small. Note that the conductivities of the transmission-line conductors may also be affected under high-pressure shock conditions.

One of the fundamental problems is that the motion must be measured close in to the device. Since the device is effectively a point source, the spherical divergence of the flow will be rather severe. For obvious noise considerations, the shorted transmission line was chosen to be coaxial in geometry. Figure 2 shows a cross section of this geometry. Here r_1 and r_0 are the radii of the inner and outer conductors respectively. For the case of the shorted transmission line, f_g is independent of z and

$$L' = \mu_0 f_g$$

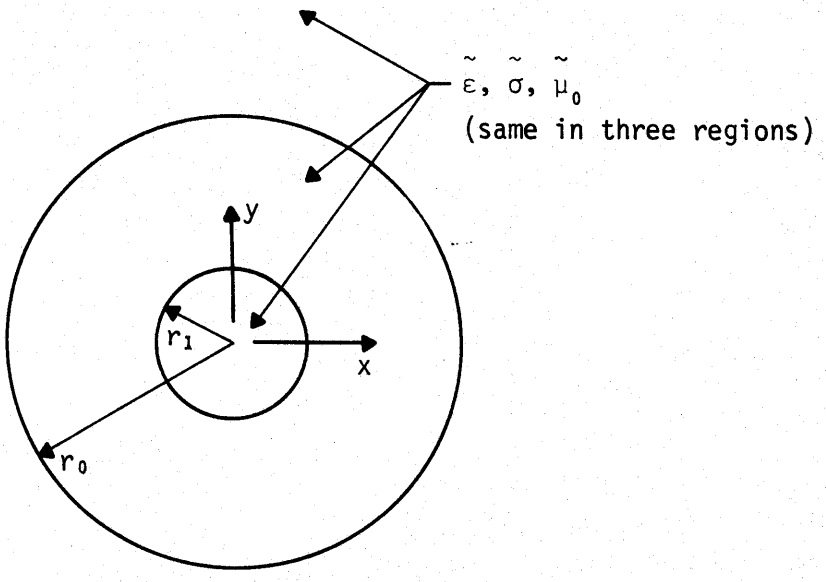

Figure 2. Circular coaxial cylindrical conductors.

In the case of the coax under uniform spherical divergence with the expanded radii r_1' and r_0',

$$r_1' = r_1 \frac{z + \Delta z}{z}$$

and

$$r_0' = r_0 \frac{z + \Delta z}{z}$$

where Δz is the radial change in distance from the center of the explosion. Thus for the case of the coax

$$f_g = \frac{1}{2\pi} \ell n \left(\frac{r_0}{r_1}\right) = \frac{1}{2\pi} \ell n \left(\frac{r_0'}{r_1'}\right) \tag{12}$$

or the inductance is independent of the effects of spherical divergence.

The extension to off-axis planar flow is a much more complex problem (Ref. 2) but is probably a second-order effect. This means that the gage will still be sensitive to changes in its length. It measures this change only along one axis.

There is one other fundamental limitation having to do with frequency response associated with this and all particle motion gages. Suppose it were desirable to sense an instantaneous step change back, a distance ℓ, in a conducting medium. If sensing, using some input drive, then the propagation goes as $e^{-2\gamma\ell}$. Since, as in Equation 5

$$\gamma = \sqrt{s\mu(\sigma + s\varepsilon)} = s\sqrt{\mu\varepsilon}\sqrt{1 + \frac{\sigma}{s\varepsilon}}$$

which through binomial expansion can be shown to be approximately equal to

$$\gamma = s\sqrt{\mu\varepsilon} + \frac{1}{2}\sigma\sqrt{\frac{\mu}{\varepsilon}}$$

or

$$e^{-2\gamma\ell} = e^{-2s\sqrt{\mu\varepsilon}\ell}\, e^{-\sigma\sqrt{\frac{\mu}{\varepsilon}}\ell} \tag{13}$$

Noting that $1/\sqrt{\mu\varepsilon}$ is the EM wave propagation velocity, the first exponential on the right side of Equation 13 is simply a time delay term. The second exponential is an attenuation term. Using an extreme case*

$$\sigma = 100 \frac{S}{m}$$

$$\mu = \mu_0 = 4\pi \times 10^{-7} \frac{H}{m}$$

$$\varepsilon = 10\varepsilon_0 = 0.885 \times 10^{-10} \frac{F}{m}$$

$$\ell = 1 \text{ m}$$

in which case

$$e^{-\sigma\sqrt{\frac{\mu}{\varepsilon}}\,\ell} = e^{-11916} = (e^{2.3})^{-5180} = 10^{-5180}$$

Thus, in this high conductivity case, one might possibly be able to observe a step change back 1 m into a conductive medium after the delay time, but it would be down 5000 orders of magnitude.

In the mid-sixties the EMP community was interested in testing buried structures. Since earth is somewhat conductive, there was some concern about this problem. In Reference 3 it is shown that there is a characteristic diffusion time (t_ℓ) associated with fields on finite length transmission lines. This is

$$t_\ell = \frac{\mu\sigma\ell^2}{4} \tag{14}$$

This implies that for an instantaneous step change in a conductive medium an observer a distance, ℓ, away would see an apparent rise time in the signal of the order of the diffusion time.

---

3. Baum, C. E., "A Transmission Line EMP Simulation Technique for Buried Structures," *Sensor and Simulation Notes*, Note XXII, June 1966.

*Note $Z_0 = \sqrt{\mu_0/\varepsilon_0} \simeq 377\ \Omega$.

Using the previous assumptions for conductivity and distance equal to 1 m, then

$$t_{\ell} = \frac{4\pi \times 10^{-7} \cdot 100 \cdot 1^2}{4} = \pi \times 10^{-5} s$$

or roughly 30 μs. This implies that the best frequency response that can be observed is of the order of 12 kHz for the case of 100 S/m and 1 m.

SUMMARY

There is a need that was established with CANT to measure the early time energy coupling into the ground from a nuclear device. While plans for CANT no longer exist, experiments on other tests should, if successful, meet the requirement. To be successful, particle motion and stress must be measured close in to the device and survive for a relatively long time (200 to 300 μs).

The FDR is a gage that is being developed for this application. It is a shorted coax transmission line whose inductance is proportional to its length. Thus a measurement of its inductance is equivalent to a measurement of displacement versus time, until the whole gage is engulfed in the shock wave. To function correctly it should be excited at a frequency whose wavelength is long compared to the gage length. As with all gages trying to transmit through a medium, the conductivity of the medium affects both the accuracy and frequency response of the measurement. The primary limitation of this gage is that the conductance of the metal path in the coax must be large in comparison to the path through the shocked dielectric.

This theory was tested. In conjunction with this, the method of measuring the inductance is described along with the subsequent HE testing of the gage.

II. INDUCTANCE MEASUREMENT

The problem has been reduced to the measurement of the self-inductance of a shorted coaxial transmission line. Recalling the excitation wavelength consideration, the length is finite. When the shock front reaches the terminals of the transmission line, the measurement is over. Several approaches can be considered. One such technique would use the simple case of self-inductance as part of an LC oscillator with a (slowly) time-varying frequency output:

$$f(t) = \frac{1}{2\pi}\,\omega(t) = \frac{1}{2\pi}\,[L(t)C]^{-1}$$

This frequency might be directly recorded after transmission via cable, or it might first be converted to an analog signal proportional to $f(t)$. Other types of reactive networks can be combined with $L(t)$ to give a different dependence of $f(t)$ on $L(t)$; if $f(t)$ is known, then $L(t)$ can be found through the designed relationship. Note that the period of $f(t)$, i.e., $f(t)^{-1}$, and the response time of the oscillator to follow changes in $L(t)$ should be small compared to times of interest in following $L(t)$. Another technique would make $L(t)$ part of a voltage divider with a reference inductance, L_r, or a more general impedance, $\tilde{Z}_r(s)$. Then, with the loading cable from the sensor and the reference impedance (including source impedance), the signal at the recorder can be used to infer $L(t)$ from the time-varying voltage-divider ratio at the operating frequency, f, again with f^{-1} sufficiently small. A more sophisticated version of this technique would have $L(t)$ as one arm of a bridge so that the initial RF amplitude going away to the recorder is essentially zero compared to the source signal, except for some small offset; as $L(t)$ decreased, the RF signal to the recorder would increase and could be amplitude-discriminated. A direct reflection technique could also be used in which an RF signal would be transmitted down a cable to the sensor and reflected back from the input port of the sensor. By having the source impedance the same as the cable characteristic impedance, the reflected wave can be terminated at the source. Then, by sampling the signal on the cable, the standing wave properties as a function of time can be determined to obtain both phase and amplitude of the reflection as a function of time. Alternatively, the

reflected signal could be sampled via a directional coupler. The magnitude as a function of time is directly obtained. By comparing the sampled reflected signal with a sample of the source signal, phase can also be obtained; or if desirable, real and imaginary parts of the complex phasor reflection can also be generated.

This latter method was actively considered early in the program and it was at this time that the transducer was dubbed the FDR. As will be seen, this may be somewhat of a misnomer in that a quadrature method of determining the real and imaginary components of a low impedance transducer at the end of a 50-Ω line was chosen. It was decided that this was easier than trying to precisely track phase due to the low impedance of the measurement. Perhaps the gage should have been simply called the particle motion gage or something of that nature. However, during the same period it was pointed out that the FDR looks like the time domain reflectometer, or TDR. They both have shorted coaxes at the end of a cable. It is with physical appearance that the similarity ends. The name FDR points out the difference and this difference is in frequency. In this case beauty goes as the skin depth. The FDR is a low-frequency device and, as previously pointed out, the coax behaves like a pure inductance. It thus uses magnetic coupling. The TDR is a high-frequency device that uses electric (and magnetic) coupling. The response is subject to the change in permittivity under shock. It is realized that some claim this change to be a constant. For the TDR the changing permittivity may or may not be a constant; for the FDR, it is comparatively irrelevant.

Suppose the gage were modeled as shown in Figure 3. The gage itself is a small resistance (R) and inductance (L) in series. It is driven by an oscillator that holds the current (i) at a continuous A sin ωt. If the voltage at the gage (V_g) is then measured, it will be

$$V_g = iR + L \frac{di}{dt}$$

or

$$V_g = AR \sin \omega t + A \omega L \cos \omega t \qquad (15)$$

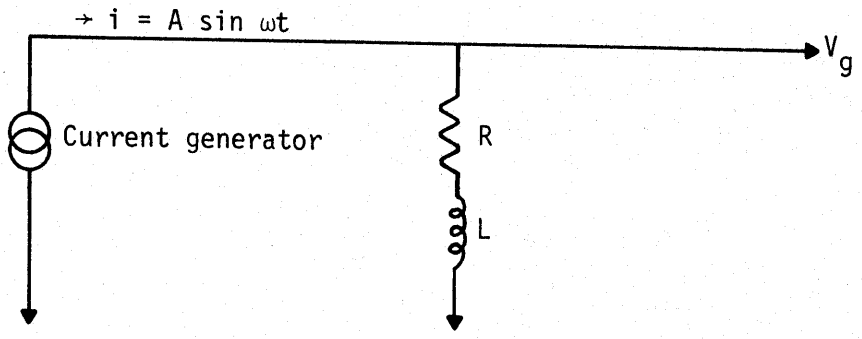

Figure 3. Simplified gage model (resistance and inductance in series).

If the input current is then sampled and used to limit the integration of the output voltages, then the resistive and inductive components can be separated as follows:

$$\int_0^{\pi} V_g \, dt = \int_0^{\pi} AR \sin \omega t \, dt + \int_0^{\pi} A\omega L \cos \omega t \, dt = \frac{2AR}{\omega} + 0 \equiv + \chi_R \quad (16)$$

and

$$\int_{-\frac{\pi}{2}}^{\frac{\pi}{2}} V_g \, dt = 0 + 2AL \equiv + \chi_L \quad (17)$$

Similarly, one can take the integrals over the remainder of the 2π radians defined by the current and obtain

$$\int_{\pi}^{2\pi} V_g \, dt = - \frac{2AR}{\omega} = - \chi_R \tag{18}$$

and

$$\int_{\frac{\pi}{2}}^{\frac{3\pi}{2}} V_g \, dt = - 2AL = -\chi_L \tag{19}$$

Using this quadrature method, the resistive and inductive components of the reactance can be separated. Thus, knowing the amplitude and frequency of the driving current, the average value of the inductance or resistance of the gage during the appropriate half-period of the integration can be calculated. The inductance measurement can be used to calculate the length of the gage at that point, and the resistance measurement can be used to see if any correction of the inductance output is necessary. (See Equation 11.)

This method of half-period integration leads to some consequences with respect to noise. Suppose that there is some noise component low in frequency with respect to the drive frequency, f, ($\omega = 2\pi f$). Then during the period of the drive frequency it will be a constant (D). The observed gage voltage (V_g) will be

$$V_g = V_g + D$$

This will affect the integrations used for determining the inductance as follows:

$$\int_{-\frac{\pi}{2}}^{\frac{\pi}{2}} V_g \, dt = \int_{-\frac{\pi}{2}}^{\frac{\pi}{2}} V_g \, dt + \int_{-\frac{\pi}{2}}^{\frac{\pi}{2}} D \, dt = \chi_L + \pi D \tag{20}$$

and

$$\int_{\frac{\pi}{2}}^{\frac{3\pi}{2}} V_g \, dt = \int_{\frac{\pi}{2}}^{\frac{3\pi}{2}} V_g \, dt + \int_{\frac{\pi}{2}}^{\frac{3\pi}{2}} D \, dt = - \chi_L + \pi D$$

If these results are combined through subtraction the result is

$$\chi_L + \pi D - (-\chi_L + \pi D) = 2\chi_L = 4AL \tag{21}$$

The result is independent of the low frequency noise. The same is true for the resistance. Thus the combination of the two results allows for the elimination of noise low in frequency with respect to the drive.

Now observe what happens to noise that is high in frequency with respect to the drive. Here it is simply observed that the integration process removes the effects of all but a half-cycle (at most) of the higher frequency.

The sources of noise could be an external EM field, or they could be generated in the gage dielectric itself (i.e., piezoelectric or triboelectric).

It should be noted that the inductance measurement is a measure of the length. If the data gathering process is interrupted by a burst of noise, the inductance measurement following would still be a measure of the length at that time. The output is not dependent on maintaining a full time history of the record. For example, the gage output is not dependent upon a continuous knowledge of both the position and velocity of the gage end.

When the gage dielectric is shocked the resistance of the gage may go down. Since this introduces a parallel component in the resistances with respect to the inductance, this is one of the prime reasons for doing the resistance measurement. The equivalent circuit with the resistance parallel to the inductance can be calculated. If R_p and L_p are the parallel components of the resistance and inductance, then they are in terms of the series resistance (R) and the series inductance (L)

$$R_p = \frac{R^2 + (\omega L)^2}{R}$$

$$L_p = \frac{R^2 + (\omega L)^2}{\omega^2 L} \qquad (22)$$

Because the gage was designed to use a 50-Ω source (large compared to the gage) for the drive, it was natural to use current as the phase reference and interpret the measurement as series equivalent values.

The last point is the frequency response that can be expected out of the data. In addition to the limit discussed in the introduction (Equation 15), it should also be noted that the sampling of the drive frequency occurs four times in each cycle: twice for the inductance and twice for the resistance. The two values are then combined to give a single value to each cycle for the inductance and resistance. This is a digital process. Thus, using the Nyquist criterion, the highest component in the data will be 0.5 f, where f is the sample frequency, or in this case the drive frequency. The Nyquist frequency is the maximum frequency attainable; a more normal criterion would be 0.2 f.

This method of measuring both the inductance and resistance of a coax is in theory quite simple. The electronics used to accomplish this are not. The first thing to choose when designing a system in the drive frequency. This is really quite simple if the frequency response requirement is known. The requirement set by the participants was 100 kHz. This mandates, according to the discussion in the previous paragraph, that the drive frequency be at least five times the frequency response requirement, or at least 500 kHz. The discussion in the introduction indicates that the lower the frequency, the better the measurement. Thus, if 500 kHz is the minimum required frequency, it is the chosen frequency.

Using this frequency, the output voltage is integrated over a period of π radians based upon the input current. There are four of these integrals, one overlapping in each period. Two of the integrals give voltages that are proportional to the inductance or length. The other two are proportional to the resistance of the sensor.

A block diagram of the circuits is given in Figure 4. The major circuit divisions are the excitation circuits, the timing circuits, and the measurement circuits. The excitation circuits condition the gage drive signal and pick off a phase reference signal. The timing circuits create precise quarter-cycle timing intervals that can be shifted in time with respect to the phase reference signals. The measurement circuits implement the half-cycle integration described in the preceding mathematical analysis.

The data are valid at the end of the integration interval. At that time the data (an analog level) are transferred to a sample-and-hold circuit. After transfer, the integrator is reset to zero and the cycle starts over. The waveforms found at various points in the circuit are shown in simplified form in Figures 5a, b, and c. Point A is the input current used to trigger the integration. Point B is the switched gage voltage. Point C is the integrated output voltage which is sampled and held and then reset at $\pi/2$ radians after the integration.

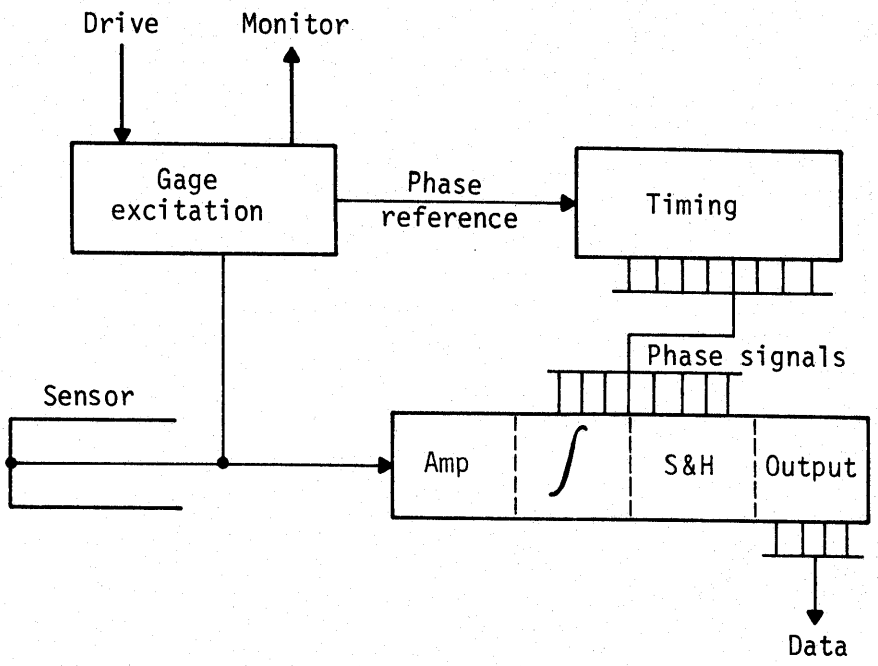

Figure 4. Block diagram of electronics.

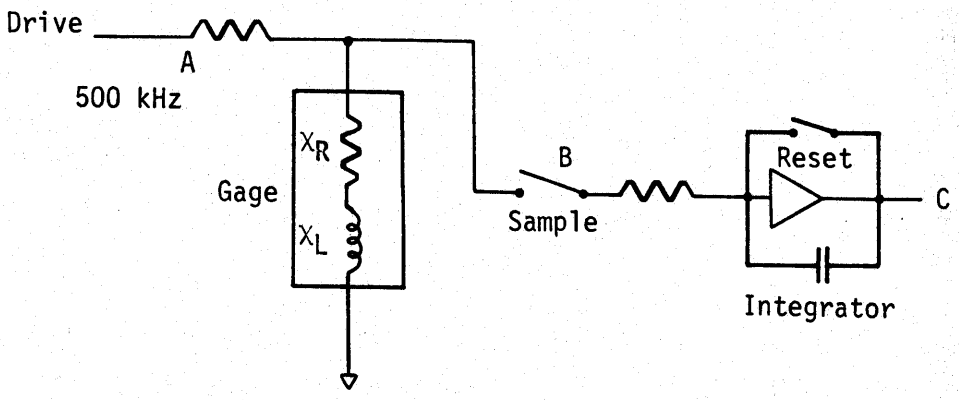

a. Simplified single channel circuit

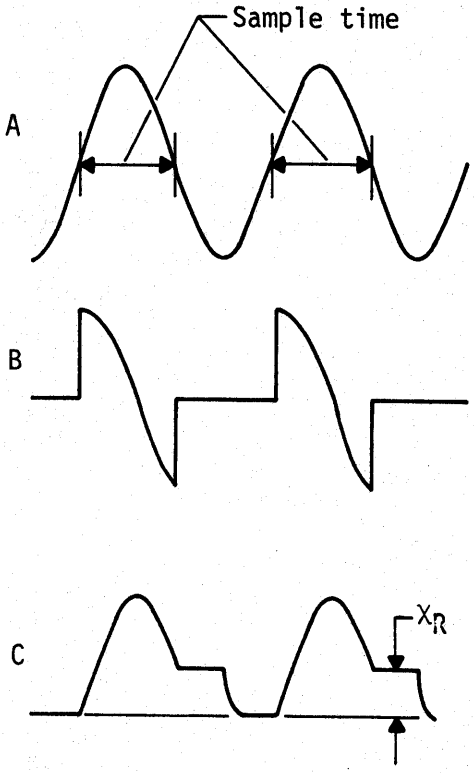

b. Resistance waveform

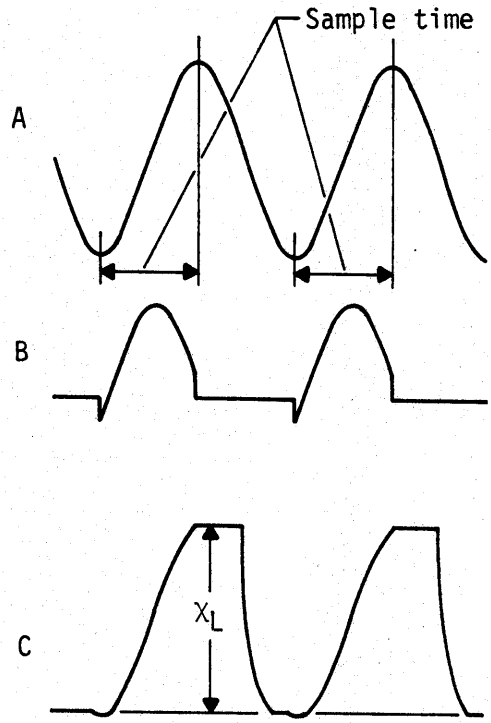

c. Inductance waveform

Figure 5. Sample waveforms.

A more detailed diagram of these electronics, designed and structured at Summers Engineering, Inc., is given in Appendix A. This shows the salient characteristics of one of the channels.

A photograph of the actual electronics package used is shown in Figure 6. The FDR main electronics were housed in an aluminum, hermetically sealed box which was 330 by 229 by 127 mm. The box houses two channels which monitor the response of two independent gages. Twenty-two BNC connectors are mounted on the box. Each channel has a 500-kHz input and 500-kHz output to the gage, and a gage signal input. Other connections on the box include phase control, gage return (not used), 500-kHz drive monitor, and four outputs marked $\pm\chi_L$ and $\pm\chi_R$ with the two remaining BNC connectors used for ± external power.

Each channel is a single PC board (102 by 254 mm). A 2.4-m cable assembly is used for hookup between the gage and the box. The PC board is comprised of four circuits: 1) drive conditioning (which monitors the 500-kHz input drive), 2) squaring amplifier (a pickoff from the drive for a phase reference for the exact timing), 3) timing network (which supplies properly timed pulses for the switches that sample the input from the gage), and 4) the data measurement network (which converts the input from the gage to d.c. voltages proportional to the χ_L and χ_R of that gage). These are discussed in more detail below.

The reader may logically ask, "Why a 2.4-m cable?" This (as will be seen later) places the electronics in a rather severe shock environment. Indeed, referring again to Figure 6, this is the reason for the steel box and foam padding shown with the electronics in Figure 6. If the cable changes its effective length, due to temperature, radiation, or whatever, this then will be reflected in the measurement. The gage is merely a shorted coax which is connected to this cable. The input current and gage voltage are sampled in the electronics package. A planned way of overcoming this difficulty is given in Section IV.

The drive conditioning circuit is diode-protected and utilizes three terminal regulators for the + and - voltages, which are set to ±7 V for external input power of ±12-20 V d.c. The load current per channel in its idle state with the gage connected is approximately 200 mA.

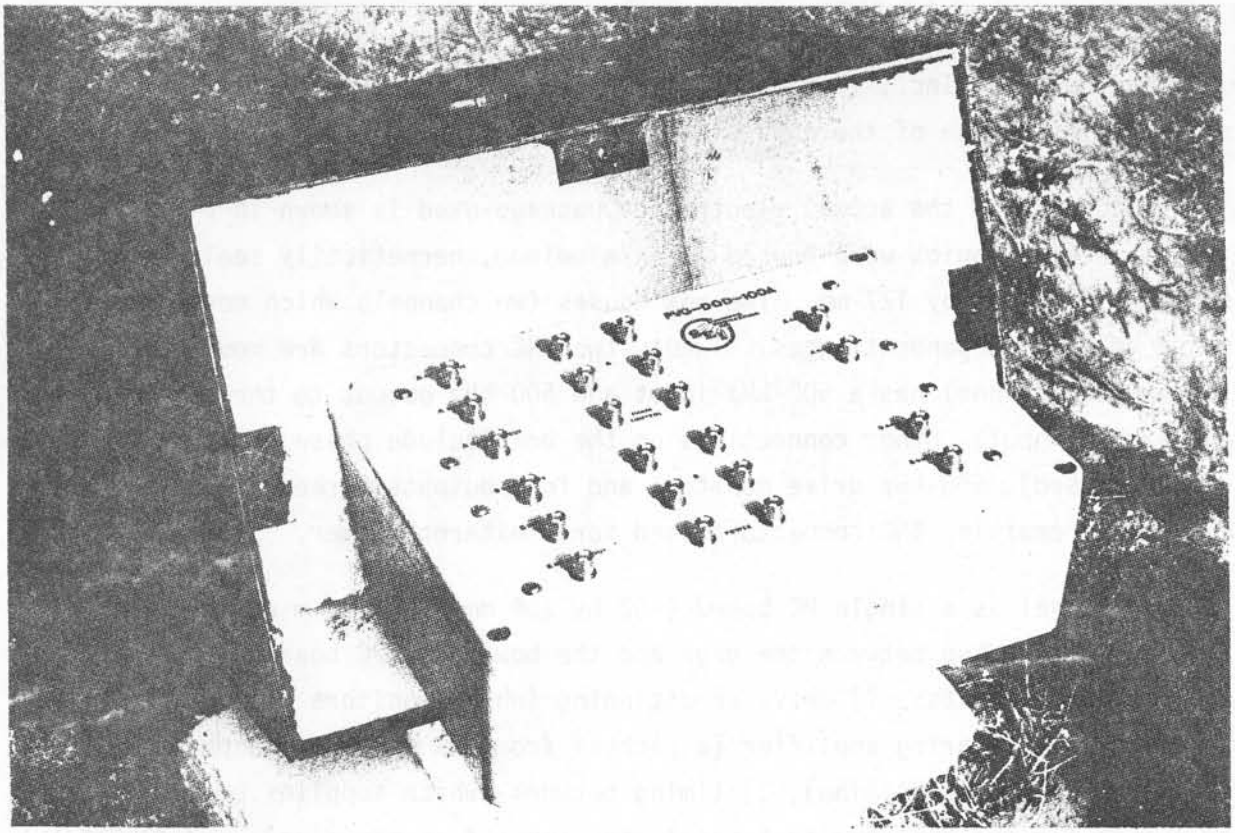

Figure 6. FDR electronics package.

The reference monitor gives a d.c. output proportional to the drive if the input drive is 10 V peak-to-peak, ±30 percent. This is done through transformer-coupling into a wideband amplifier stage, to peak detection with diodes, and an output amplifier stage that drives a 50-Ω load.

The squaring amplifier, which provides phase reference, is transformer-coupled to the drive. A differential amplifier, used for sine to square wave conversion, is transformer-coupled to an integrator which gives a triangle wave output. This triangle wave is used to set timing, which is critical in extracting the χ_L and χ_R values.

The timing network is needed to drive the switching in the data measurement network. A CMOS phase lock loop (PLL) runs at four times the reference frequency (500 kHz). A counter is used as a divide-by-four for shift register drive. The shift register has eight outputs equally loaded for balance in timing. The phase control from the triangle output of the squaring amplifier is skewed for setting zero phase.

The data measurement network extracts the χ_L and χ_R values in the following manner: The signal returned from the gage is amplified by a factor of 5, using a wideband operational amplifier. The amplified signal is then applied to four identical circuits that integrate, sample, hold, and reset. Timing of the four circuits is 90 deg apart. This is accomplished by three sections of a CMOS switch and an operational amplifier. A second operational amplifier, with the aid of two transistors, gives a gain of 10 and the ability to drive 50-Ω loads.

An assembly drawing for the gage is shown in Figure 7. As can be seen it is a perforated* aluminum (6061-T6) tube 50 cm long with an ID of 50.8 mm and an OD of 57.15 mm. The center conductor is also an aluminum tube with an OD of 6.35 mm and a wall thickness of 1.65 mm. A GR connector was used to connect the cable and the gage. The connector provided a low resistance, reliable connection--not an impedance match.

*Note that for comparison two of the gages were not perforated.

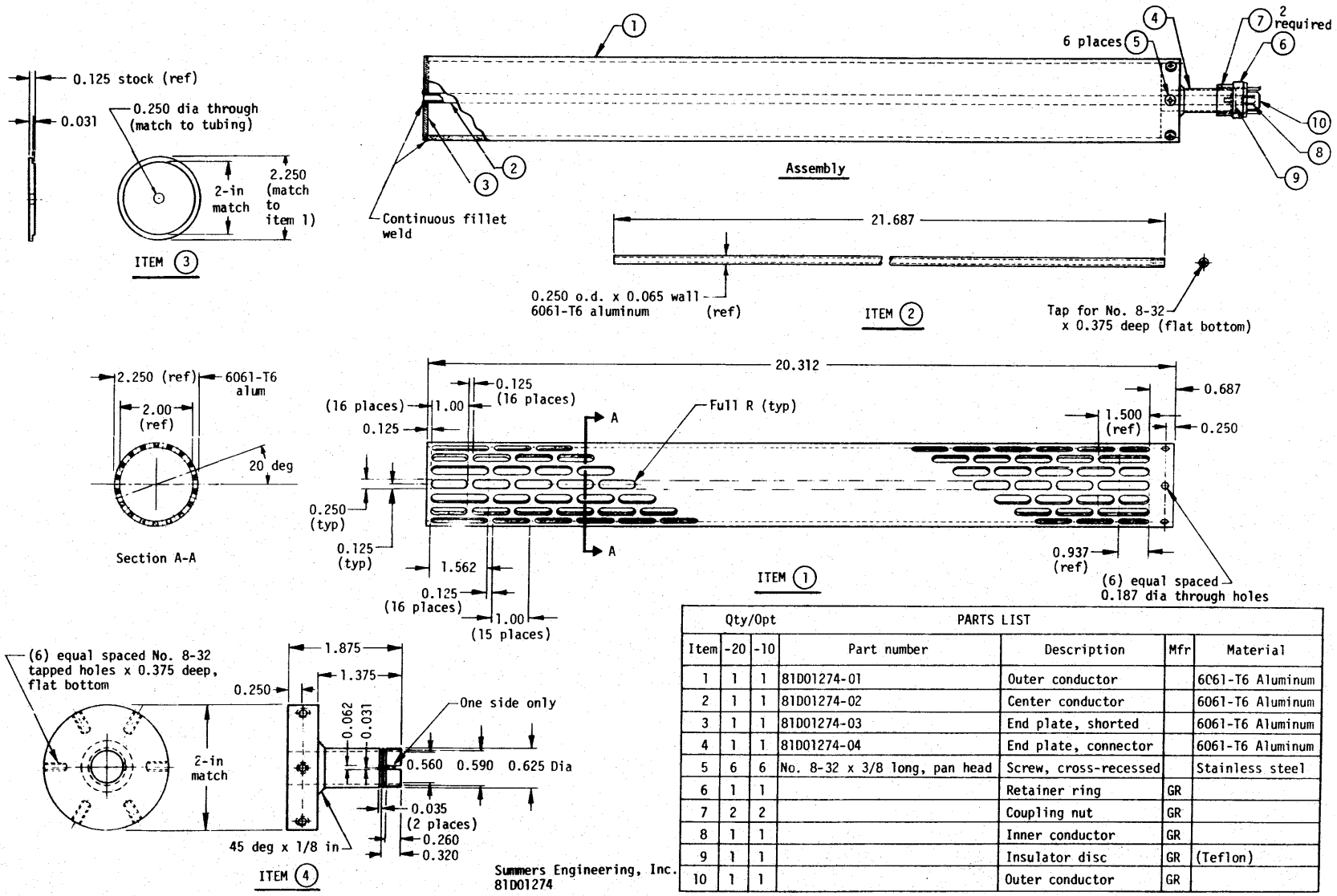

Item	Qty/Opt -20	Qty/Opt -10	Part number	Description	Mfr	Material
1	1	1	81D01274-01	Outer conductor		6061-T6 Aluminum
2	1	1	81D01274-02	Center conductor		6061-T6 Aluminum
3	1	1	81D01274-03	End plate, shorted		6061-T6 Aluminum
4	1	1	81D01274-04	End plate, connector		6061-T6 Aluminum
5	6	6	No. 8-32 x 3/8 long, pan head	Screw, cross-recessed		Stainless steel
6	1	1		Retainer ring	GR	
7	2	2		Coupling nut	GR	
8	1	1		Inner conductor	GR	
9	1	1		Insulator disc	GR	(Teflon)
10	1	1		Outer conductor	GR	

PARTS LIST

Figure 7. FDR gage.

The center tube was filled with epoxy (Epon 828). Two different dielectrics were used. One was epoxy; the other was to coat the gage with epoxy and fill it with 2C4 grout. This grout is a tuff matching grout that had a density of 1.76 g/cm^3. Its composition is given in Table 1.

TABLE 1. 2C4 TUFF MATCHING GROUT COMPOSITION

Weight, %	Ingredient
32	Type 1 portland cement
21.5	Plaster sand[a]
20.5	Berite
2.8	Bentonite
0.078	CFR 2
Balance	Water

[a]The original formula called for 20-40 Monterey sand, but plaster sand was used to be consistent with work being done at SRI International.

In summary, although inductance could be measured in a number of ways, a quadrature method was chosen which measures both the inductance and resistance of the transducer. The operating frequency was a comparatively low 500 kHz.

III. HE EXPERIMENTS

TEST SETUP AND CALIBRATION

Four HE experiments were conducted during September 1981. The purpose of these experiments was to verify the concept of the FDR as discussed in the previous two sections. The philosophy behind these experiments was to subject the gage to a high stress shock loading and see if the response behaved in a predictable manner.

Each of the four tests contained two FDR gages. Each gage was 50 cm long and 50.8 mm ID (Fig. 7). In the first three tests the gages were perforated; in the last test they were not. In each test one FDR gage had an epoxy dielectric and the other gage was coated with a thin layer of epoxy and filled with 2C4 grout. The gages were mounted symmetrically with respect to center (102 mm apart*) and secured in a cardboard casting tube (Fig. 8).

Four piezoelectric TOA pins were also mounted with the gages. The first pin was at the surface and the next two were mounted behind the first pin at depths of 6 and 12 mm. The fourth pin was placed at 25 cm.

The 406-mm-diameter form was then filled with 2C4 grout to a depth of approximately 50 cm. The shorted ends of the FDR gages were 6 mm from the surface.

After a 7-day cure the gages were tested at the McCormick Ranch test site south of Kirtland Air Force Base. The high explosive consisted of a nominal 41 kg of Composition C-4 plastic explosive. C-4 is a military explosive which has a detonation velocity of 8.04 km/s and a density of 1590 kg/m^3 (Ref. 4). The explosive was packed into a 305-mm-diameter cardboard tube and set upon the grout block containing the FDRs. This HE experimental configuration is shown in Figure 9. The explosives and sample were then bermed over in preparation for the tests. In the first two tests the explosive was ignited with a

---

4. Dobratz, B., *Properties of Chemical Explosives and Explosive Simulants*, UCRL-51319, Rev. 1, July 1974.

*With the exception of test 4, where the gages were mounted on 135-mm centers.

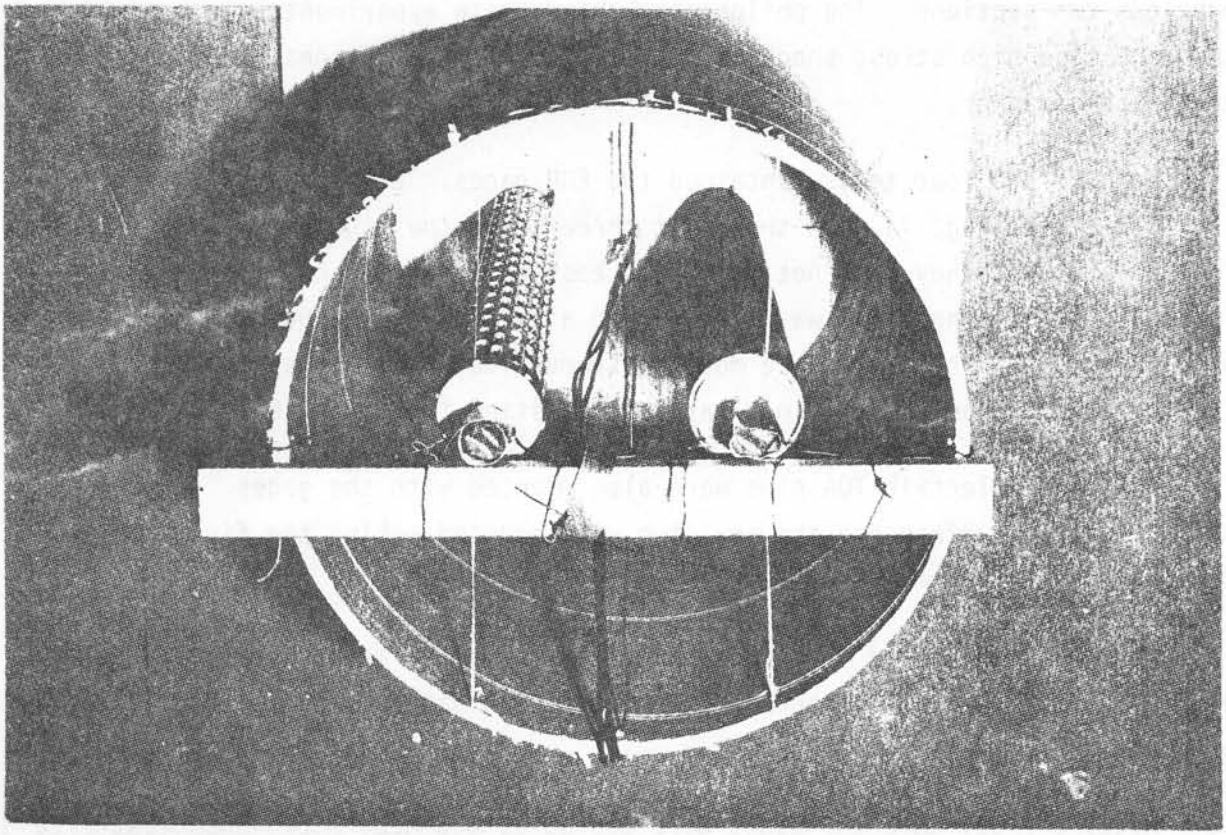

Figure 8. FDR gage test emplacement.

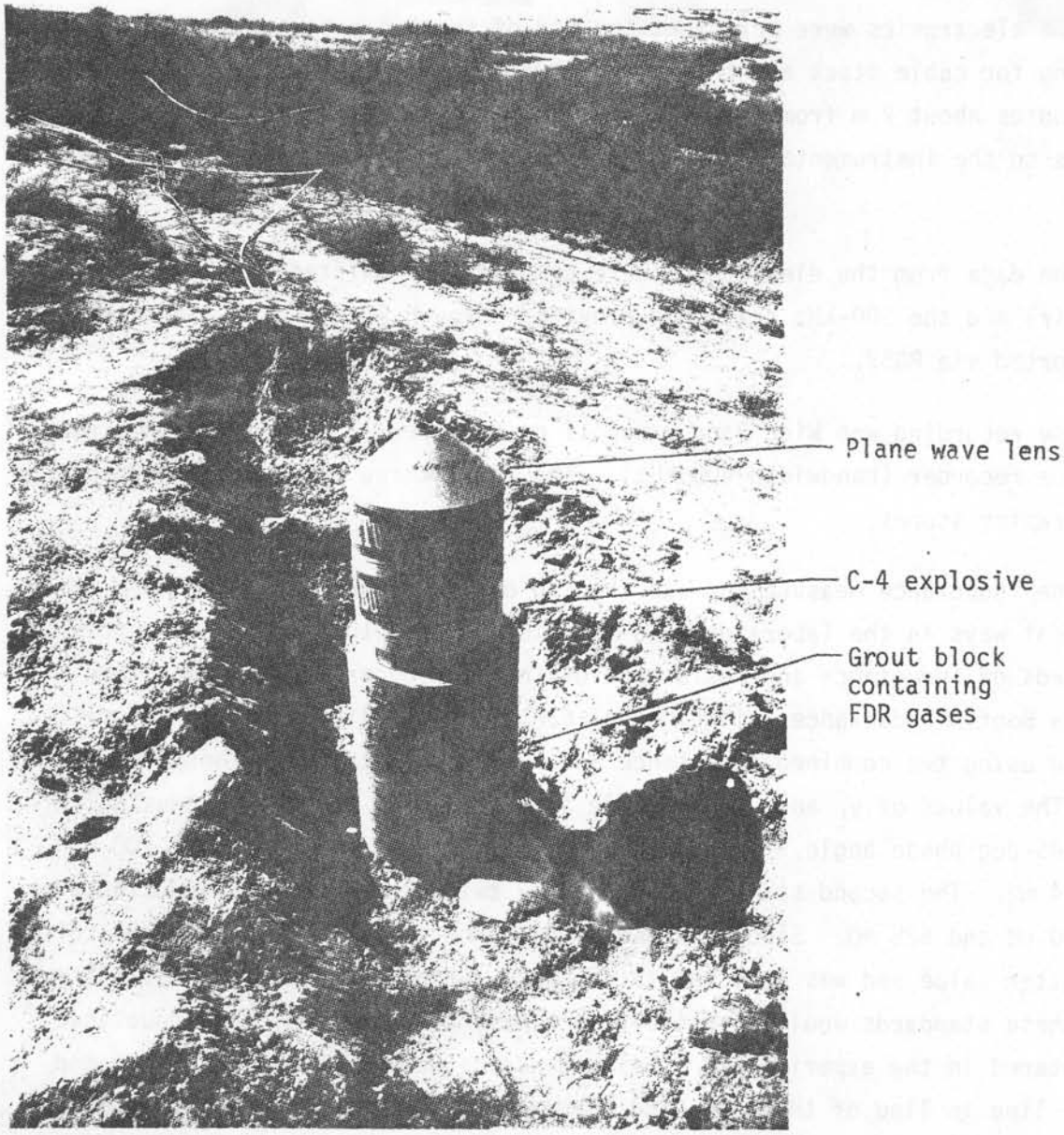

Figure 9. McCormick Ranch HE test of FDR.

P-80 (203-mm-diameter) plane wave lens. During the last two tests a P-120 (305-mm-diameter) plane wave lens was used.

The electronics were buried at the end of the 2.4-m connecting cable. Allowing for cable stack and the fact that there were two gages placed the electronics about 2 m from the explosive. The cables connecting the electronics to the instrumentation van where the data were recorded were 150 m long.

The data from the electronics were carried over twisted shielded pairs (20 pair) and the 500-kHz drive was provided through RG331. The pin data were transported via RG58.

The recording was Wide Band Group II on an Ampex 2230 twenty-eight channel tape recorder (bandwidth 400 kHz). The first three pins were recorded using raster scopes.

The inductance measurement was checked out and adjusted in a number of different ways in the laboratory and the field before the shot. Laboratory standards of inductance and resistance of the transducers were established using a Booton Inductance Bridge, Model 63H. Field calibration was accomplished using two combined inductance and resistance standards constructed at SEI. The values of χ_L and χ_R were made to be equal at 500 kHz, producing an exact 45-deg phase angle. One of the standards had an inductance of 100 nH and 314 mΩ. The second standard was exactly twice these values--inductance was 200 nH and 628 mΩ. Since the gage inductance is approximately equal to the latter value and was expected to decrease during the test, it was felt that these standards would adequately encompass the values of the inductance encountered in the experiments. These standards were then placed at the end of the line in lieu of the gage, and the system was then adjusted to give correct and consistent readings. Following this procedure a dummy gage was installed. This was a 50-cm sliding shorted air line similar in dimensions to the finished gage. The shaft that moved the short was metered in length. It was then moved known amounts, and the output was checked for consistency and correctness. This process varied the inductance through the range of 15 to

225 nH. The system was then further checked using a General Radio adjustable air line Model 874-LK20L and a General Radio Short, Model 874 WOL. This produced a calibration of the output voltage at the recorder versus the inductance and resistance at the gage. The tape deck was calibrated using a Bell & Howell TCS-2000 as a voltage standard. The net result of the process was a calibration of absolute voltage outputted at the tape recorder versus the resistance and inductance.

RESULTS

The first test was fired on September 9, 1981. The results of this shot were at first somewhat confusing but later were enlightening as to the gage performance. In these tests the $+\chi_L$ signal from the gage was expected to go negative in voltage, signifying a decrease in length, and the $-\chi_L$ signal was expected to increase in value. For this reason the system saturation was set close to the baseline. In the case of the $-\chi_L$ signal, the baseline was set close to the lower band edge. The $+\chi_L$ was set close to the upper band edge to increase the effective dynamic range of the instrument.

The results of the inductance measurements are shown in Figure 10. Figure 10 shows a signal that is at first negative going and saturates the electronics. This signal should have been a monotonically increasing function. Figure 10a on the other hand should have been a monotonically decreasing function. In Figures 10c and 10d the opposite phenomenon occurs. The same type behavior was shown in the resistance. The only difference between the two is the dielectric used in the gage. One gage was epoxy coated and grout filled. The other was epoxy filled. It was then postulated that this effect was due to a low frequency noise produced in the gage itself, probably by the dielectric and probably piezoelectric in nature.

On the next test this hypothesis was checked. The current drive to the gage was doubled to double the signal-to-noise ratio. These data are shown in Figures 11a and b. The low frequency noise is still present and with the same sign as before. However, this time the data do not go to saturation. Thus, if Equation 21 is correct, a calculation of the displacement can be made.

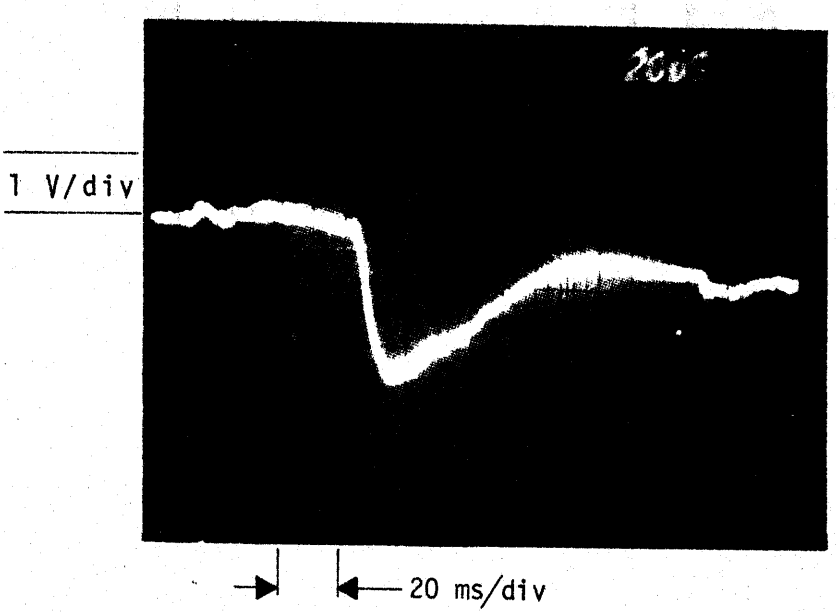

a. χ_L grout dielectric.

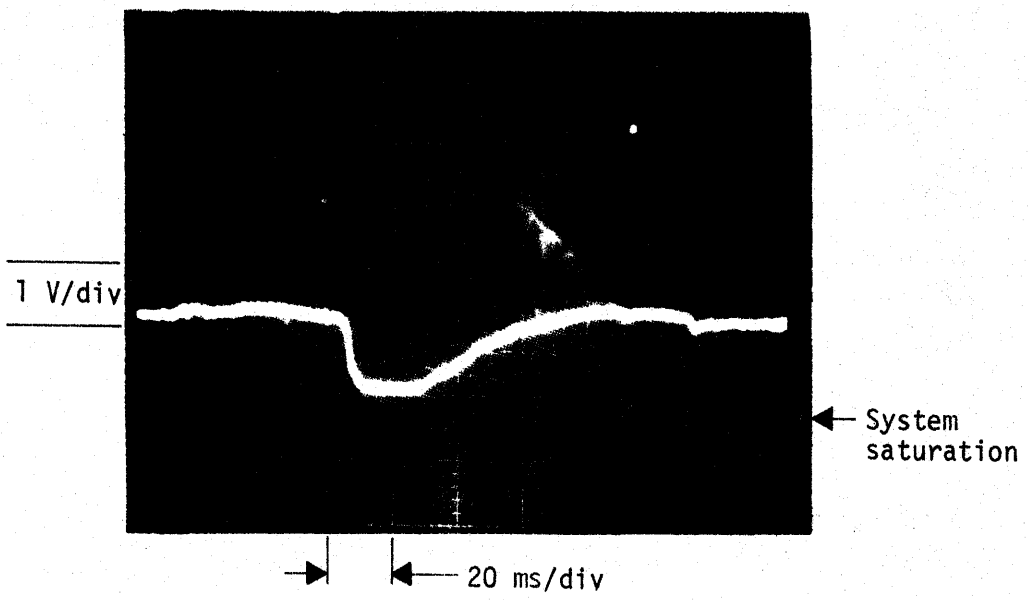

b. χ_L grout dielectric.

Figure 10. Inductance measurements on FDR Shot 1.

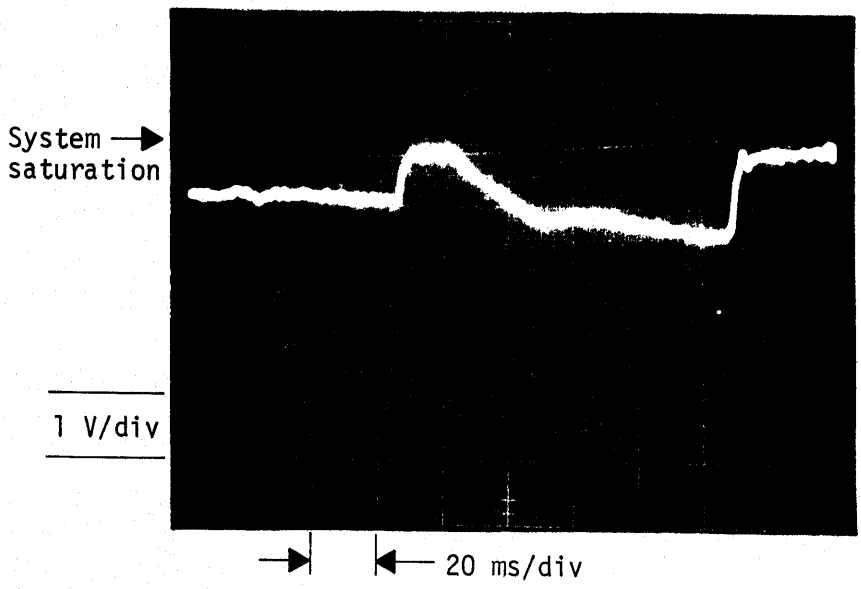

c. χ_L epoxy dielectric.

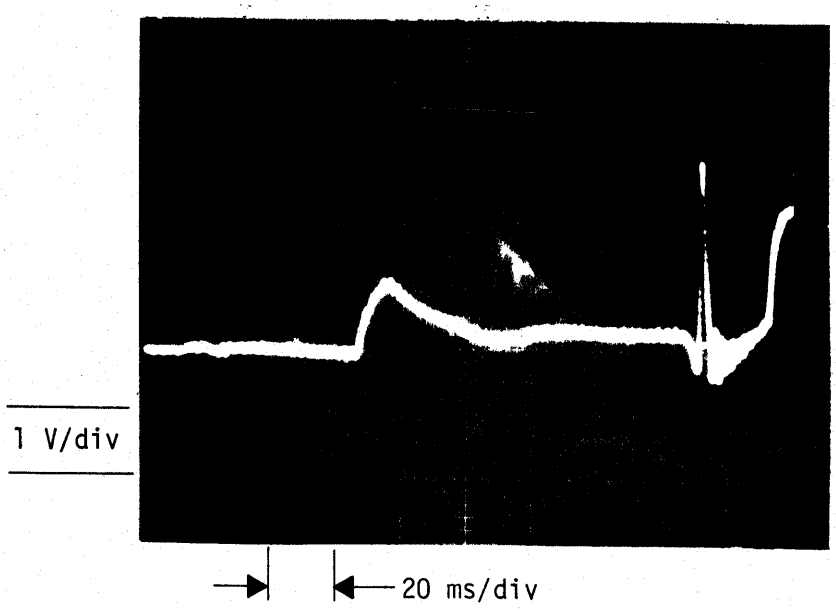

d. χ_L epoxy dielectric.

Figure 10. Concluded.

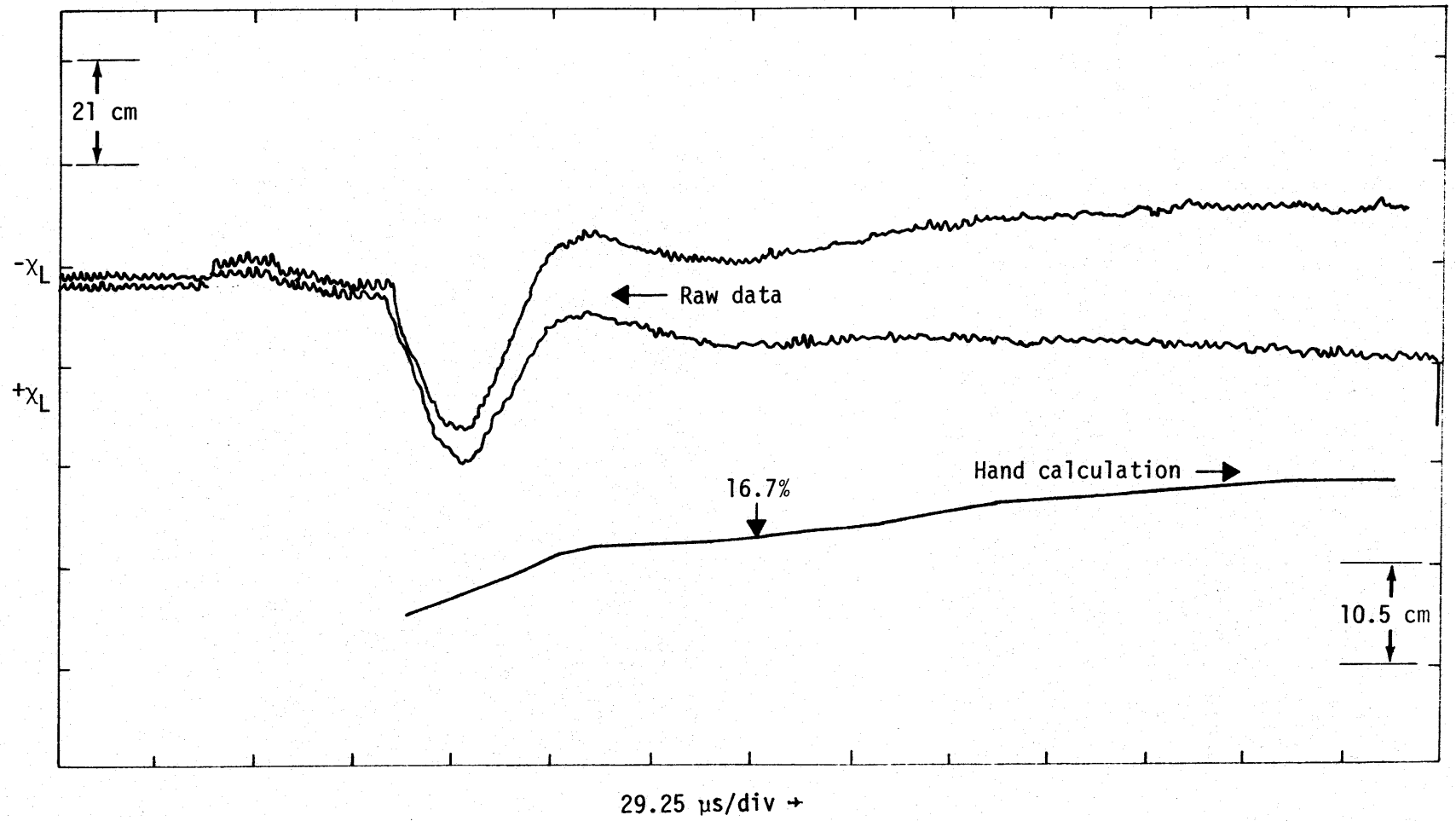

a. Grout dielectric.

Figure 11. Test 2 raw inductance data and hand-calculated displacement.

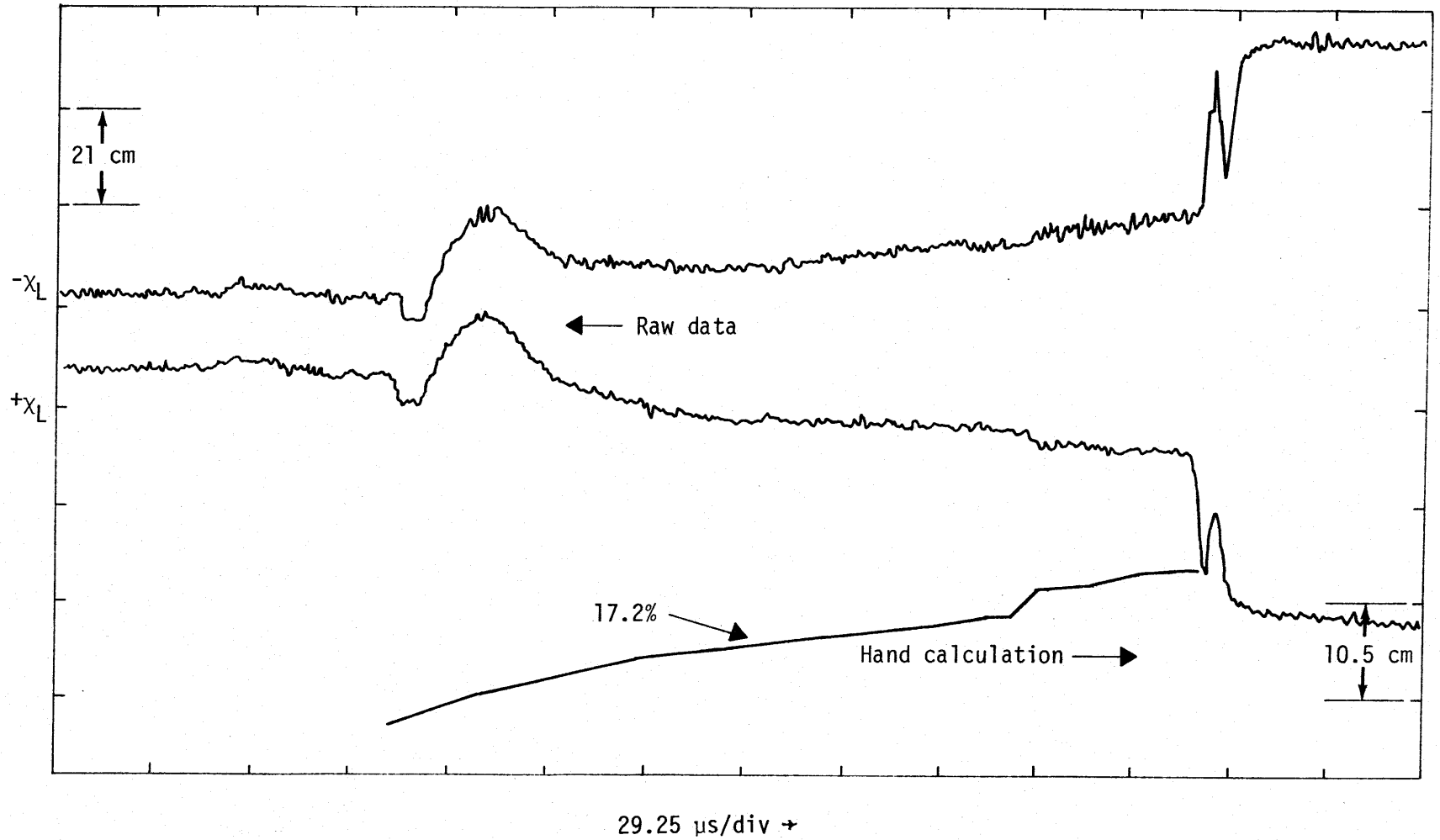

b. Epoxy dielectric.

Figure 11. Concluded.

As an example, the grout dielectric FDR had a measured length of 50.24 cm. It had a measured inductance of 223.3 nH. The connector had an inductance of 9.87 nH, or the coax had a self-inductance of 214.4 nH. Its sensitivity to displacement was therefore 4.268 nH/cm. The field calibration measured the difference of the two standards at 100.3 nH. On the $+\chi_L$ channel this corresponded to a difference of 0.853 V. On the tape channel for $+\chi_L$, 1 V corresponds to 0.523 V out. Thus for $+\chi_L$, the inductance change (ΔL) in terms of output voltage (V_1) is

$$\Delta L_1 = \frac{V_1}{0.523} \times \frac{100.3}{0.85} = 225.09\ V_1 \qquad (23)$$

in nanohenries. Similarly for the $-\chi_L$ channel, the tape gain was 1/(0.513) and the inductance change (ΔL_2) in terms of output voltage (V_2) was

$$L = \frac{V_2}{0.513} \times \frac{100.3}{0.873} = 223.96\ V_1 \qquad (24)$$

in nanohenries. Thus the length change ($\Delta \ell$) is

$$\Delta \ell = \frac{(\Delta L_1 - \Delta L_2)}{2 \times 4.268} = 0.117\ (\Delta L_1 - \Delta L_2) \qquad (25)$$

in centimeters. The values obtained for this gage in Equations 23 through 25 will, of course, change slightly for each gage used. The data were first reduced by hand as shown in Figure 11.

It should be noted that the gage is completely engulfed by the shock wave after 120 to 170 μs after shock arrival. The data after this time should be ignored.

The data were also digitized using the same reproduce amplifiers as were used in the field. The data were filtered at 220 kHz and the digitizing was done at the rate of 1.1 MHz. The calculations were then performed using the digitized data, shown plotted in Figures 12 and 13. These calculated data were also filtered at 100 kHz using a three-pole low-pass Butterworth digital filter. Both are shown in each plot, the smoother data being filtered at 100 kHz, the nominal gage response (Section II).

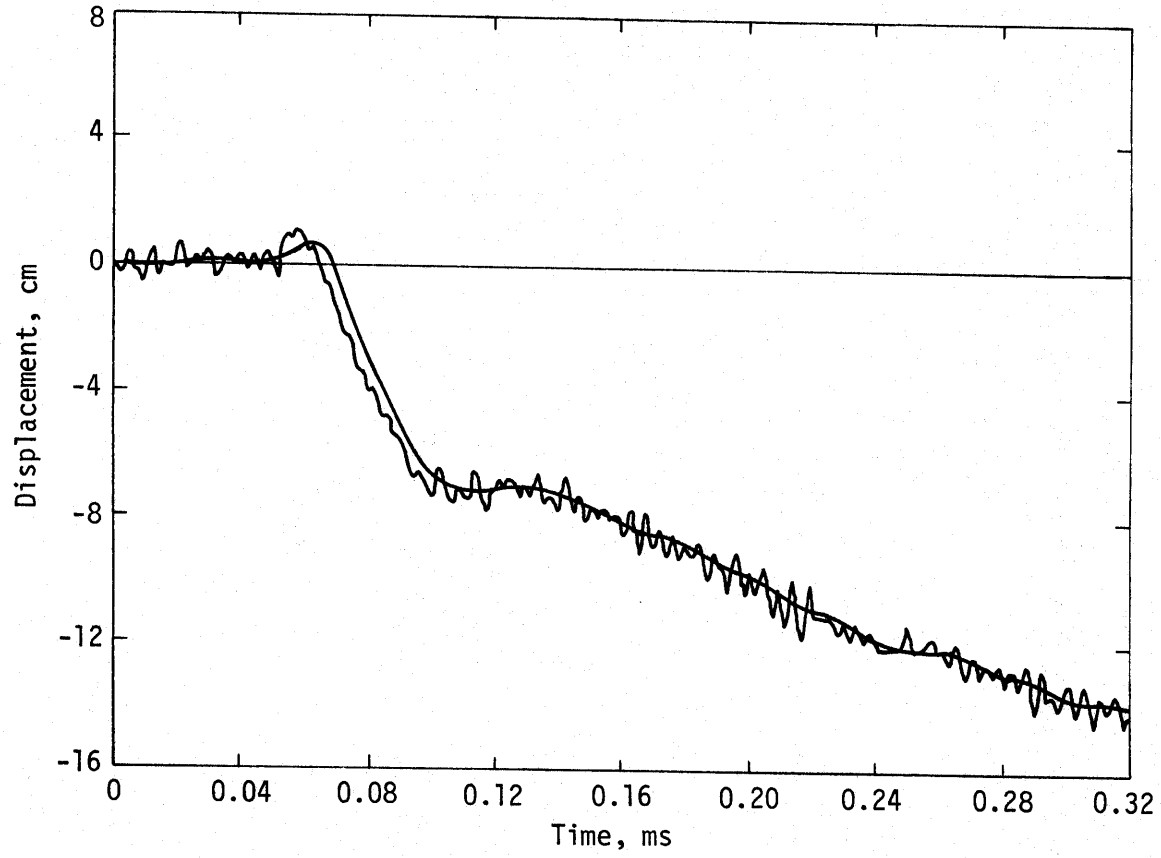

Figure 12. FDR with grout dielectric, Test 2, displacement versus time.

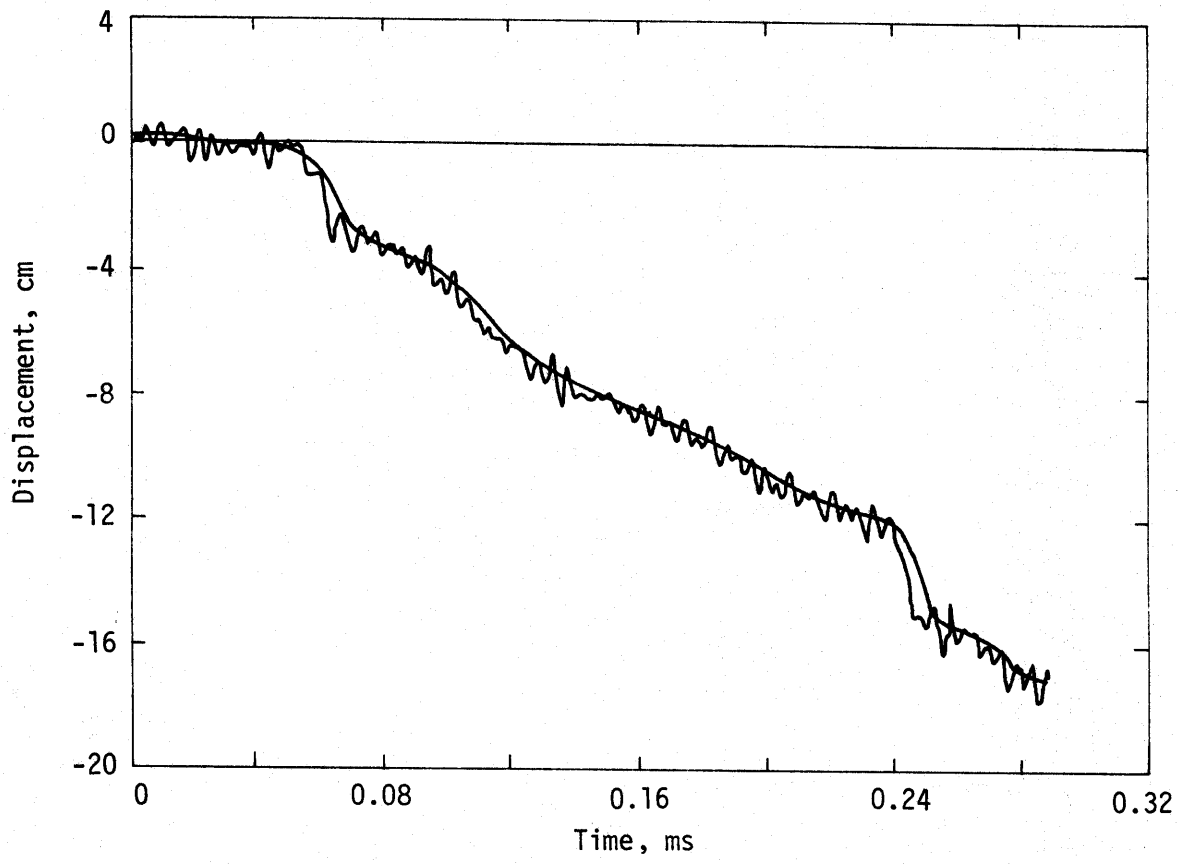

Figure 13. FDR with epoxy dielectric, Test 2, displacement versus time.

At the time it was felt that the relatively large piezoelectric noise could lead to common mode problems in the data reduction, as was the case shown in Figures 12 and 13. The early-time response differs significantly in wave shape. Additionally, as will be shown, the response differs from shots 3 and 4. This difference is probably due to common mode effects.

In order to limit the effect of this probably piezoelectric noise the output voltage from the gage was high pass filtered at 100 kHz prior to the integration. This does not affect the gage response, since the gage operates at 500 kHz with an expected response of 100 kHz; it only gets rid of the low frequency noise produced in the gage.

The raw output data obtained in this manner are shown in Figures 14a and b. It is observed that while there still may be some minor piezoelectric noise, it is extremely limited in comparison to that observed in shots 1 and 2. The reduced data are again plotted as before, in Figures 15 and 16. Again the smooth line is the low pass filtered (100 kHz) reduced data.

The electronics for shot 4 were the same as for shot 3. The only difference was that the transducers were not perforated. The reduced data are shown in Figures 17 and 18.

In all shots the resistance change was minimal. There was no apparent effect on the inductance measurement.

The shock velocity measurements did not work in shots 2 and 3 due to malfunctions of the raster scopes, due in one case to trigger failure, and in the other blooming consequent to excessive shutter opening time. The shock velocity (u_s) read had some uncertainty associated with it but appeared to be of the order of 4.25 km/s on both shots 1 and 4. This was measured in the upper 12 mm of the center of the sample.

It should be emphasized that the data taken with the FDR were particle displacement, not particle velocity. Particle velocity can be calculated from these data but extreme care must be used. It was decided to simply take the displacement 30 μs after shock arrival and use it to calculate the peak

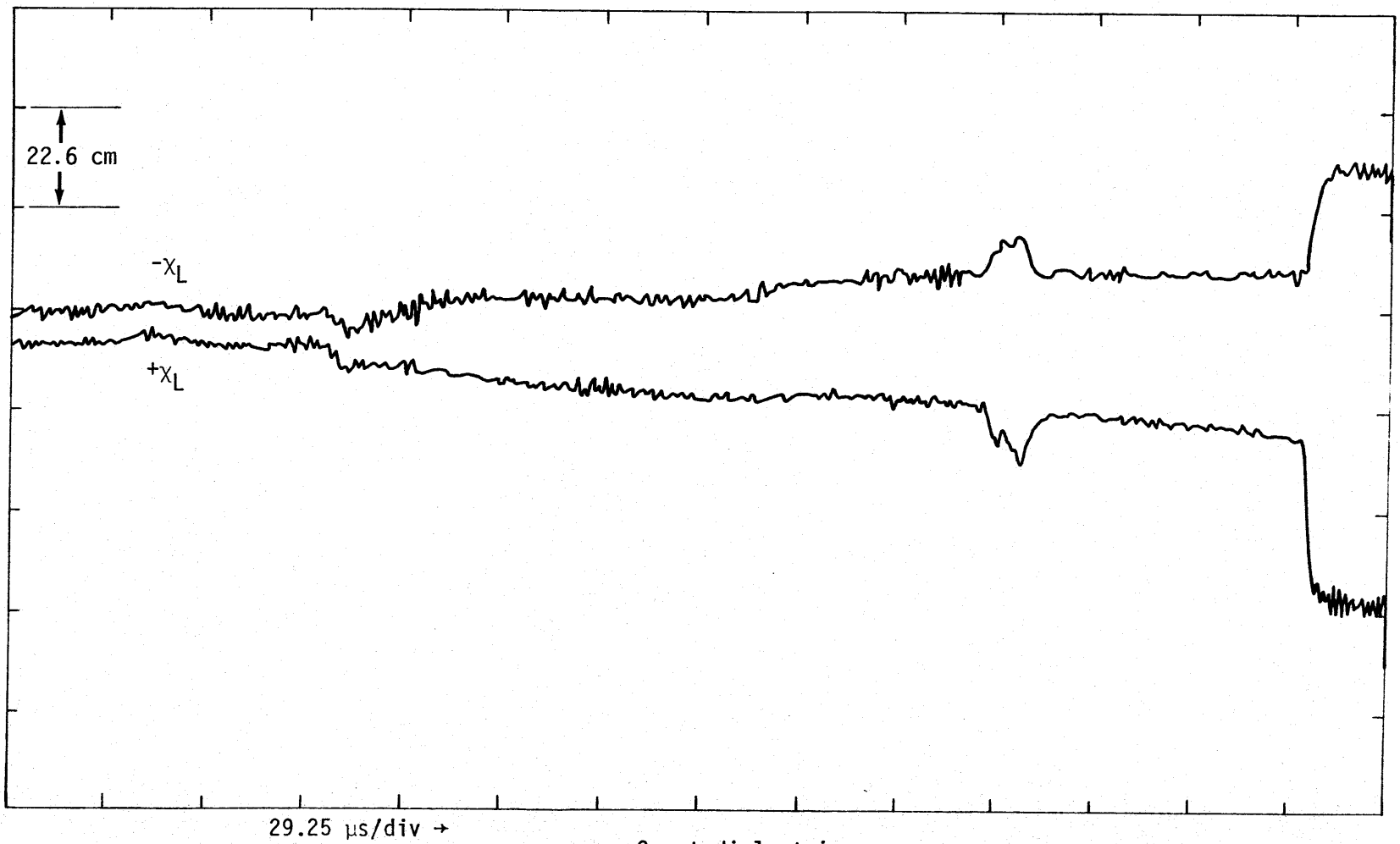

a. Grout dielectric.

Figure 14. Test 3 raw inductance data.

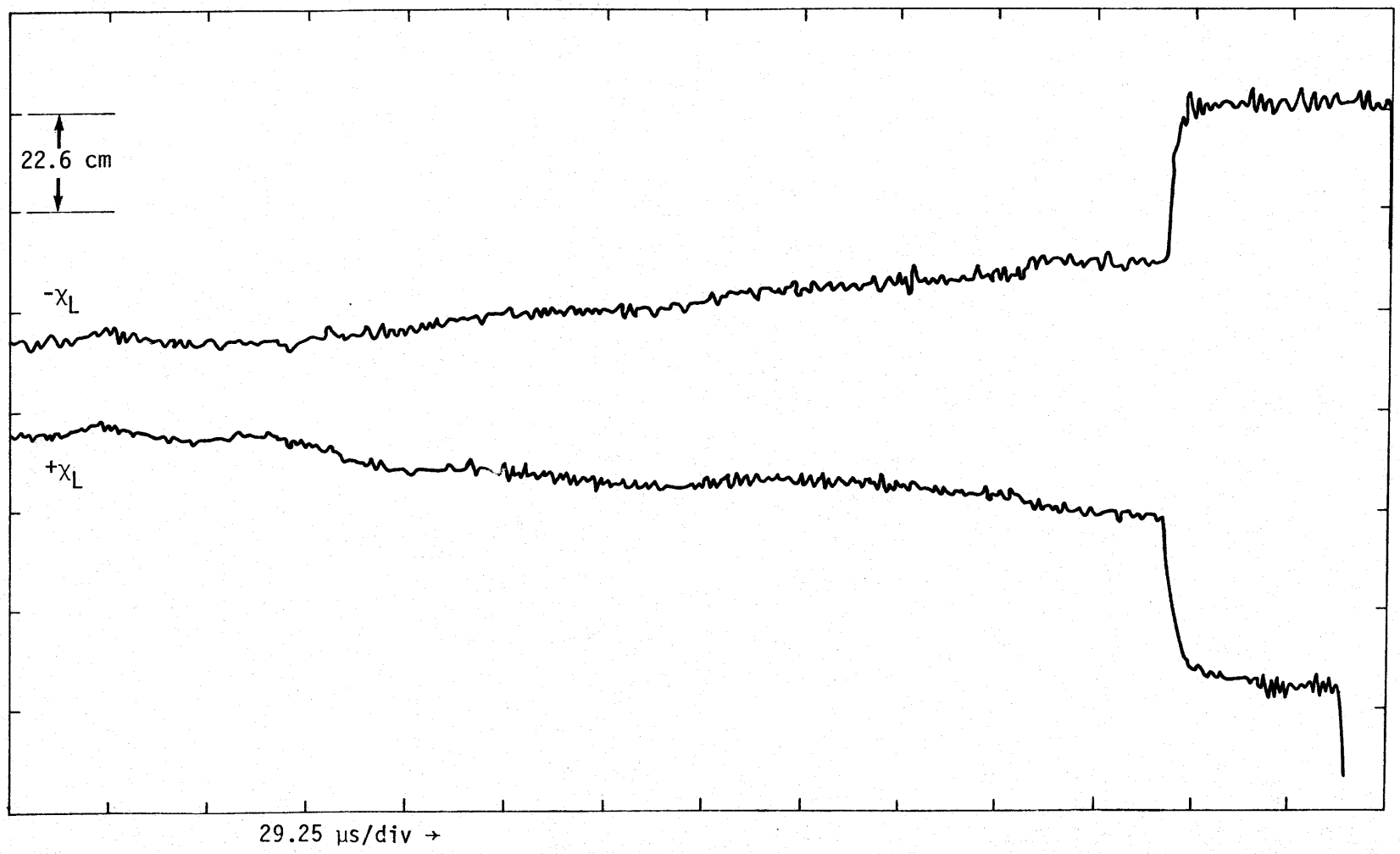

b. Epoxy dielectric.

Figure 14. Concluded.

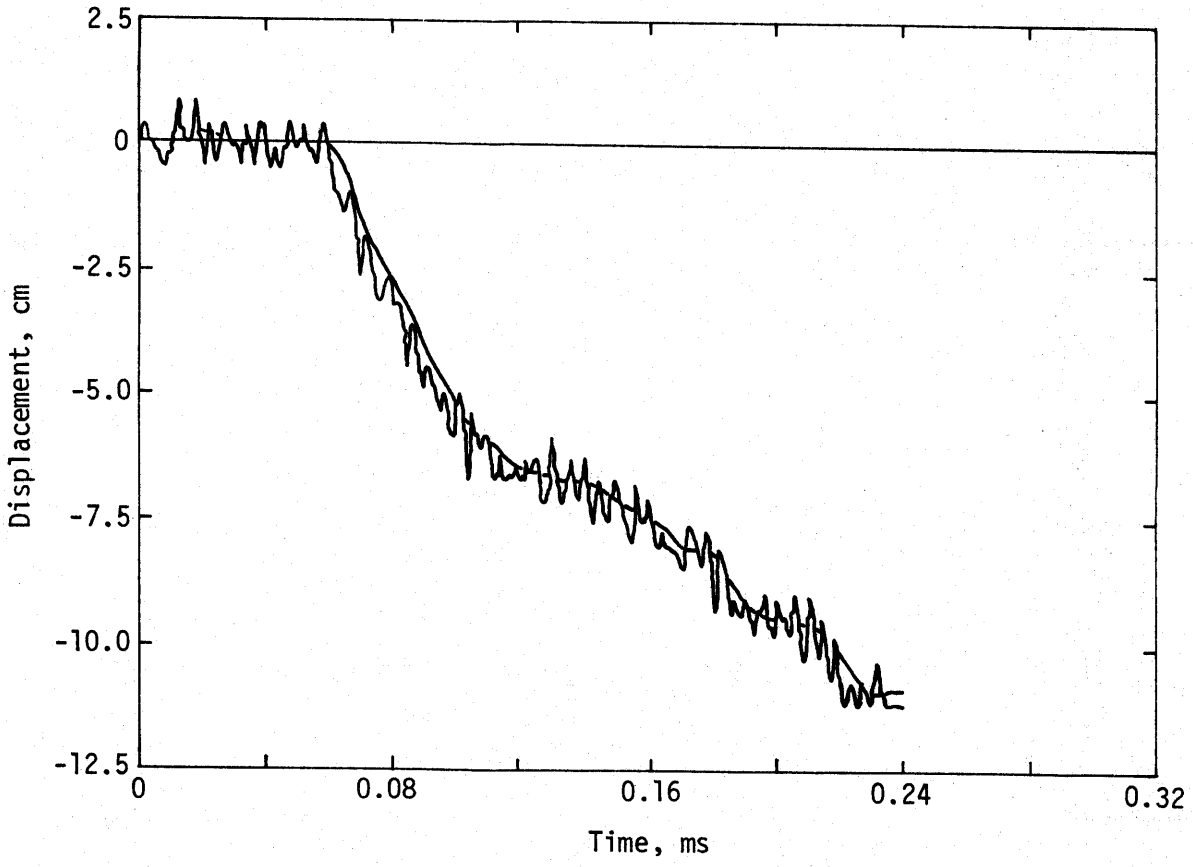

Figure 15. FDR with grout dielectric, Test 3, displacement versus time.

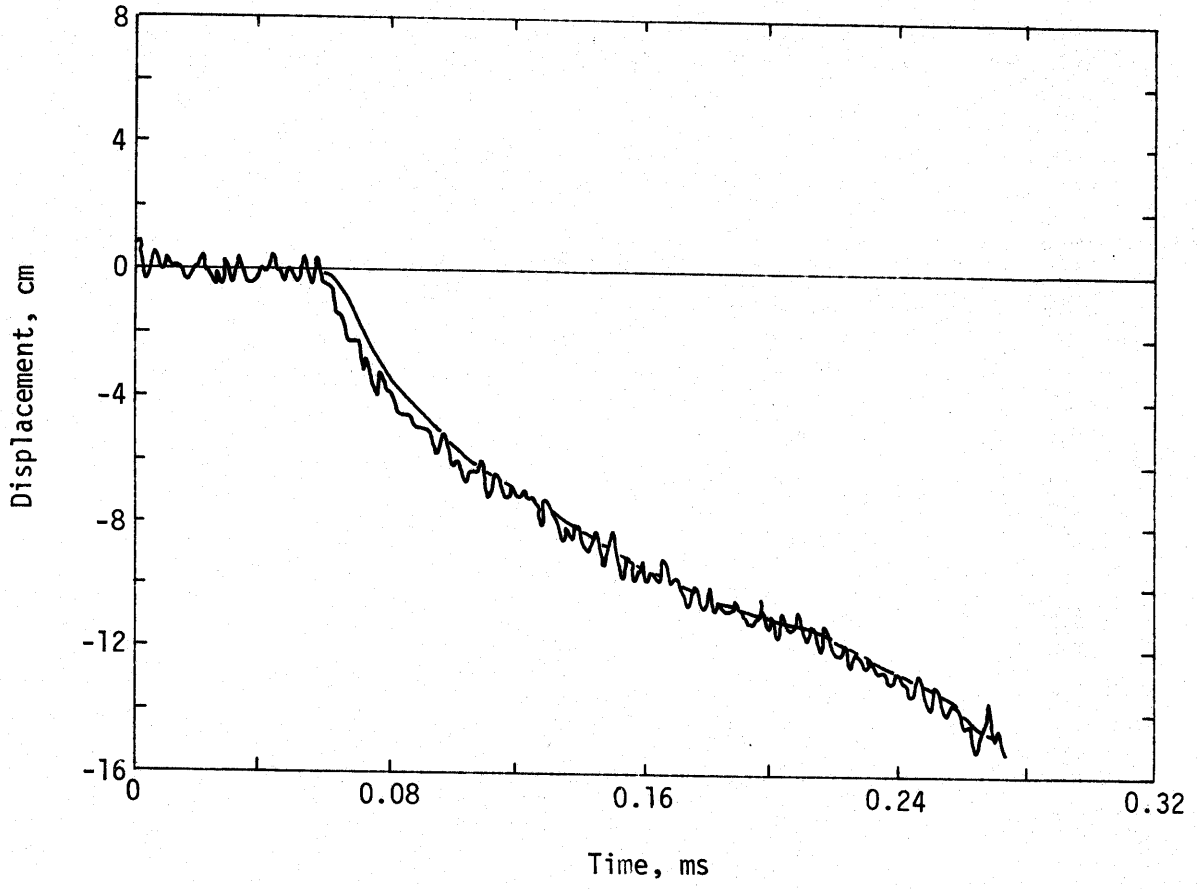

Figure 16. FDR with epoxy dielectric, Test 3, displacement versus time.

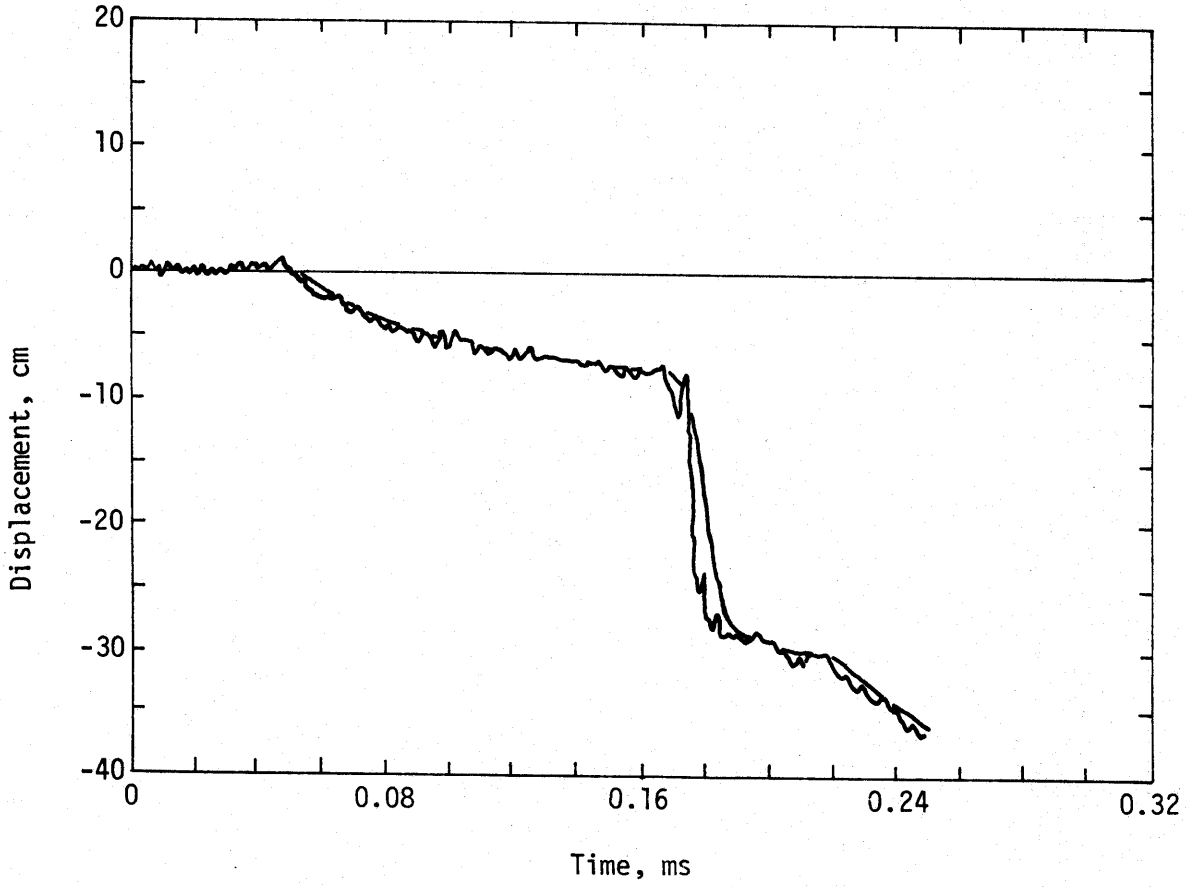

Figure 17. FDR with grout dielectric, Test 4, displacement versus time.

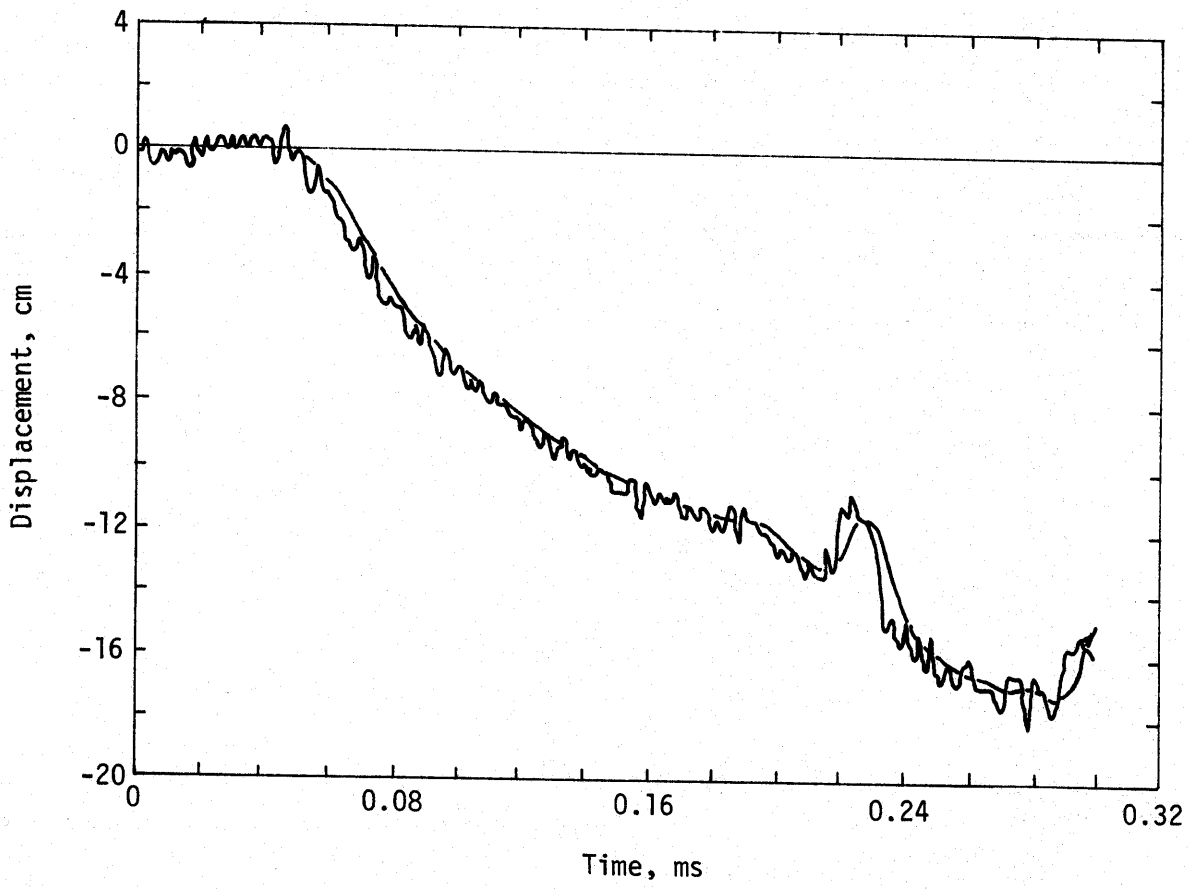

Figure 18. FDR with epoxy dielectric, Test 4, displacement versus time.

particle velocity. This 30 μs was chosen because it was the approximate time for the release wave to reach the transducer location from the edge of the explosive. The displacements were

1. Shot 3: grout dielectric--3.75 cm
2. Shot 4: grout dielectric--3.5 to 4 cm*
3. Shot 3: epoxy dielectric--4.5 cm
4. Shot 4: epoxy dielectric--4.4 cm

This corresponds to a particle velocity (u_p) of 1.25 km/s with the grout dielectric and a particle velocity of 1.5 km/s with the epoxy dielectric. The differences in particle velocity are probably attributable to the different mechanical properties of the two dielectrics.

The data can be differentiated numerically on a computer. A number of different techniques were tried (polynomial fits and sliding windows). However, while they appeared to be right in magnitude, the process of differentiation accentuates even the extremely minor noise appearing on the 100-kHz filtered data; for this reason it is not shown.

Shots 1 and 2 are not shown because of the previously mentioned problem with the probably piezoelectric noise.

Keeping in mind the uncertainty in the shock velocity measurement, the approximate peak pressure (P) can be calculated using the grout dielectric gage data and the relationship

$$P = \rho_0 u_s u_p$$

where ρ_0 is the initial density (1.76 g/cm^3 or 1760 kg/m^3). This value turns out to be 9.3 GPa. There is an additional uncertainty associated with this in that the density appeared to vary with time by about 10 percent. The lower density was used and the peak pressure could have been 10 percent greater or on the order of 10 GPa.

---

*See scale of Figure 17.

IV. CONCLUSIONS AND RECOMMENDATIONS

From this limited series of four tests, it may be concluded that a significant advance has been made in high stress particle motion gage technology. The FDR works. This is true up to the range of 10 GPa.

Conductivity does not appear to be a problem at this stress level. It may become one as the stress level increases. The mere presence of a probably piezoelectric phenomenon confirms this.

The detection of this phenomenon points out one of the basic advantages of using an a.c. technique: the noise is easily segregated from the true data. When using a d.c. technique all that can be done is to overpower it by increasing the current, a method which often causes concern with adjacent experimenters. The FDR uses a 200-mA drive current. In spite of the fact that it is planned to double this for nuclear applications, this will still be minor in comparison to the hundreds and thousands of amperes required in d.c. techniques.

The frequency used was 500 kHz. When operated at this frequency, the FDR gives a data bandwidth of approximately 100 kHz. This is felt to be adequate for the applications under consideration. This is stated with the caveat that if the conductivity of the medium increases dramatically, the frequency response as well as the whole gage performance will diminish. This should not be considered as a gross limitation of the FDR because it is true for all the high stress particle motion gages.

The FDR measurement is only one of change in length. It will only measure the flow in one direction.

The plans for further development of the gage include radiation hardening of the electronics to make them more suitable for use on an underground test.

A particular limitation of the FDR used here was that the electronics had to be close to the gage to minimize the effects of possible changes in the effective length of the cable connecting the gage and the electronics. It is planned to overcome this difficulty by using a current sampling transformer at the gage location.

The FDR used in this effort was designed as a fieldable laboratory device. It is not suitable for use on a large-scale experiment. The reason for this is that all the calibration and setup for the experiment required access to the gage and electronics. This will be overcome by automating these functions and providing a calibration step with the data. In fact, the lack of a calibration step and merely using absolute voltage caused a great deal of difficulty when reducing the data on the computer. The recommended modification should simplify this process.

When fielding on an underground test, one of the most important considerations is shielding because of the relatively intense noise environments. While the FDR is, in comparison, relatively immune from external field effects, they should still be considered. Figure 19 gives a generic shield plan for an underground test. It is a doubly shielded system terminated at both ends with To Be Determined (TBD) resistors. On a small test the recorder and electronics could be at the same locations. The possibility of making the recorder digital is presently being investigated. The integrating and sampling process for obtaining the data make this possibility attractive. The outer shield is shown as a solid conduit around the cables. When transitioning through a pressure plug, this could become a screen of some type to ensure the pressure seal. However, when this is done, care should be taken to ensure that extremely large currents are not flowing adjacent to this shield. On a large test, the electronics should be close to the gage and thus destroyed postshot. In this case, the recorder obviously will be separate from the electronics.

In preparation for underground testing, it is hoped that more material testing will be done, specifically geared toward determining the conductivity at high pressure. This affects all the gages under consideration.

The present plans are to field the modified FDR on some HE events and hopefully on some underground tests.

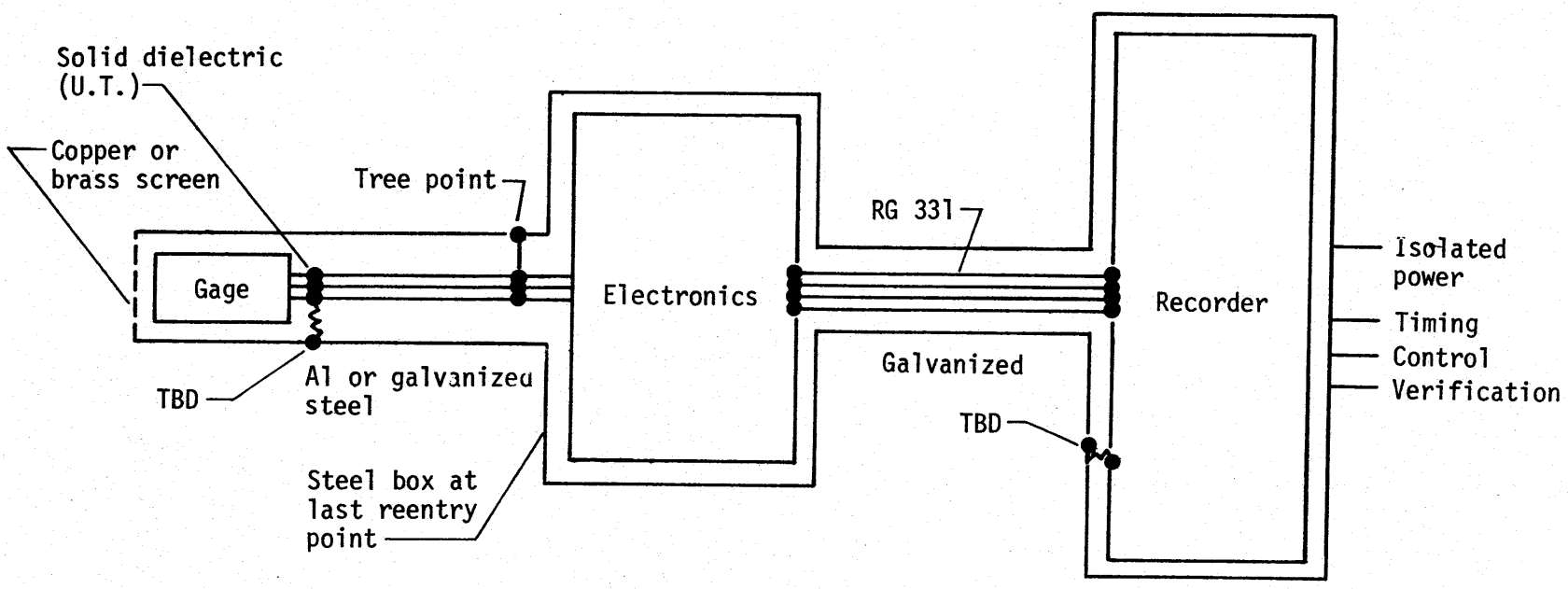

Figure 19. FDR shielding.

Thus, in summary, there is a new deal in particle motion gages. It is called the Frequency Domain Reflectometer (FDR). It is different from the other gages considered in that it uses a relatively low frequency a.c. technique to determine the self-inductance of a coaxial cable segment. We in the instrumentation community are now much closer to saying, "CANT can be done."

APPENDIX A

Functional Schematic of FDR Electronics

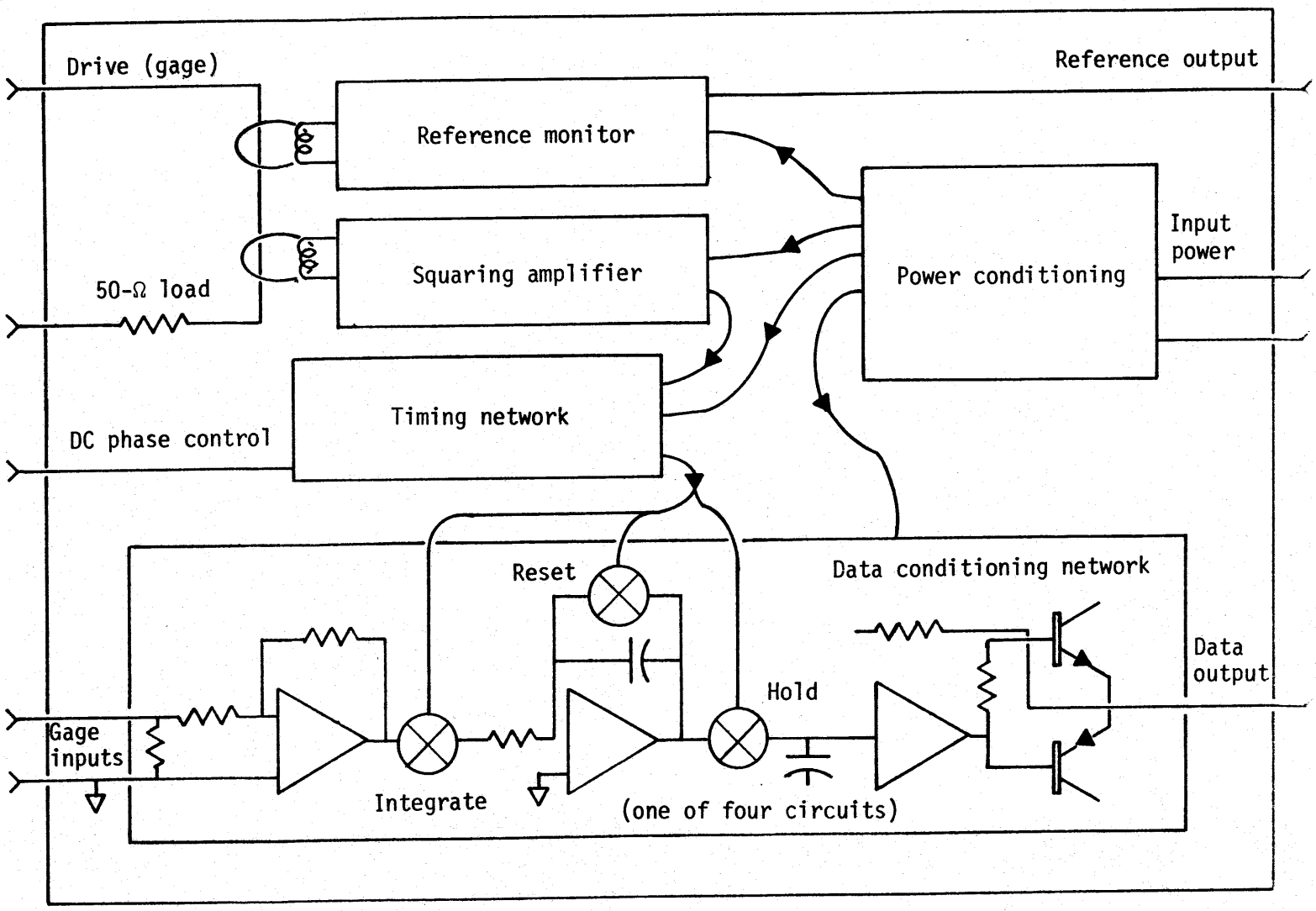

Figure A-1. Functional schematic of FDR electronics.